Applied Energy 408 (2026) 127417

Contents lists available at ScienceDirect

Applied Energy

journal homepage: www.elsevier.com/locate/apenergy

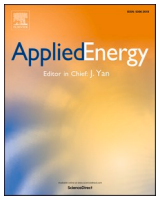

Dynamic adaptive model predictive control for prosumers-based energy communities

Pablo Horrillo-Quintero [a,c], Pablo García-Triviño [a], Sérgio F. Santos [b], David Carrasco-González [a], Luis M. Fernández-Ramírez [a,*], João P.S. Catalão [c]

[a] Research Group in Sustainable and Renewable Electrical Technologies (PAIDI-TEP023), Department of Electrical Engineering, Higher Technical School of Engineering of Algeciras (ETSIA), University of Cádiz, Avda. Ramón Puyol, s/n., 11202 Algeciras, Cádiz, Spain
[b] Research Centre for Mechanical and Aerospace Science and Technologies (C-MAST), University of Beira Interior, R. Fonte do Lameiro, 6201-001 Covilhã, Portugal
[c] Research Center for Systems and Technologies (SYSTEC), Advanced Production and Intelligent Systems Associate Laboratory (ARISE), Faculty of Engineering, University of Porto, 4200-465 Porto, Portugal

HIGHLIGHTS

- Novel adaptive MPC framework for prosumer-based energy communities.
- Dynamic weight and constraint tuning enable optimal mode transitions.
- Achieves 6.13–44.92% reduction in operational costs and power losses.
- Ensures 79.31% average renewable utilisation, outperforming fixed MPCs.
- Balances cost-efficiency and sustainability better than PSO approaches.

ARTICLE INFO

Keywords:
Adaptive model predictive control
Dynamic control
Energy communities
Optimisation
Renewable energy

ABSTRACT

Energy communities (ECs) offer a significant opportunity for decentralised energy production. However, realising their full potential is hindered by the significant challenge of managing the high volatility of renewable energy technologies (RETs) and dynamic electricity markets. To address this, the present work introduces a novel dynamic adaptive model predictive control (AMPC) framework designed to simultaneously reduce costs, minimise losses, and enhance RET integration in prosumer-based ECs. The methodology is built upon a high-fidelity dynamic model of the EC, operating with a 50 μs time step to accurately capture the switching dynamics of power electronics and ensure a realistic representation of system behaviour. The key innovation lies in the dynamic adaptation of AMPC weights and power constraints, enabling seamless transitions between a self-sufficiency mode during high-price periods and an economically optimised grid-interactive mode during favourable market conditions. The performance of the AMPC is rigorously benchmarked against fixed MPC strategies and the particle swarm optimisation (PSO) algorithm. The results demonstrate the profound superiority of the adaptive approach, showing reductions in operational costs and power losses of 6.13% to 44.92%, without compromising sustainability. The AMPC's average RET utilisation of 79.31% was superior to that of the fixed-MPC strategies, with improvements ranging from 0.45% to 13.34%. Furthermore, it demonstrated a highly efficient balance against the metaheuristic approach, where a minor 2.53% difference in utilisation was exchanged for significant gains in cost and efficiency. Finally, compared with an adaptive PSO strategy, it reduces 120% power losses and increases 28.33% the capacity utilisation. These results demonstrate a superior framework for achieving a cost-effective, efficient, and sustainable operation.

* Corresponding author.
E-mail addresses: pablo.horrillo@uca.es (P. Horrillo-Quintero), pablo.garcia@uca.es (P. García-Triviño), sfs@ubi.pt (S.F. Santos), luis.fernandez@uca.es (L.M. Fernández-Ramírez), catalao@fe.up.pt (J.P.S. Catalão).

https://doi.org/10.1016/j.apenergy.2026.127417
Received 16 October 2025; Received in revised form 18 December 2025; Accepted 13 January 2026
Available online 23 January 2026
0306-2619/© 2026 The Authors. Published by Elsevier Ltd. This is an open access article under the CC BY-NC-ND license (http://creativecommons.org/licenses/by-nc-nd/4.0/).

1. Introduction

Energy communities (ECs) are increasingly recognised as pivotal actors in advancing the shift towards decentralised energy systems. An EC can be defined as a local and self-organising entity that operates independently or semi-independently within a distribution network [1]. Unlike conventional centralised structures, where electricity flows unidirectionally from utility companies to consumers, ECs establish a bidirectional framework that enables community members to both produce and consume energy. Within this setting, individuals and organisations take on the role of prosumers, generating electricity—typically from renewable electrical technologies (RETs) such as photovoltaic (PV) panels and energy storage systems (ESSs) like battery ESS (BESS)—while also consuming it locally [2]. The integration of prosumers into ECs represents a fundamental shift in how energy is managed and distributed. This structure enhances energy autonomy, supports the transition to low-carbon systems, and fosters greater social engagement by enabling citizens to participate in energy production and exchange actively [3]. Consequently, the incorporation of prosumers is not only a technical innovation but also a cornerstone for achieving flexibility, sustainability, and resilience in future innovative energy systems [4].

Despite their promising potential, ECs face several challenges that must be addressed to ensure effective deployment and scalability [5]. Power losses are substantially higher in conventional centralised grids due to long-distance transmission lines [6]. By aligning energy generation with local consumption, ECs significantly reduce transmission distances and the associated resistive losses, thereby enhancing overall system performance [7,8]. A key opportunity for ECs is the development of control and optimisation algorithms that effectively reduce power losses. Moreover, a critical issue in modern power systems is mitigating environmental impacts associated with the heavy reliance on fossil fuels [9]. The integration of RETs into ECs provides a practical pathway to reduce greenhouse gas emissions and accelerate the transition to low-carbon, sustainable energy models. Nevertheless, the inherent variability of RETs such as PV panels and wind turbines may compromise the reliability of supply. To address this challenge, ECs increasingly rely on ESS, including BESS, which allows surplus generation to be stored during periods of high availability or peak demand. However, dynamic approaches are needed to faithfully capture EC behaviour and transient states, which are commonly overlooked [10]. Furthermore, the collective exchange of energy resources among nearby prosumers emerges as a promising approach to democratise access to electricity, making it more affordable, sustainable, and widely available [11]. In addition to these technical advantages, the economic dimension remains a decisive factor, as ECs help reduce energy costs for participants and strengthen the financial resilience of local communities [12].

To address these challenges, most of the existing literature has relied on stochastic and heuristic optimisation strategies, mainly through linear programming (LP), mixed-integer linear programming (MILP) [13], and genetic algorithms, which are typically constrained to hourly or daily time horizons. While effective for long-term scheduling, these approaches often fail to capture the dynamic behaviour of prosumer-based ECs, highlighting the need for more advanced control and management frameworks [14]. For instance, the study in [15] proposed a community energy management system (EMS) to address the consumer-level problem using Geofind and a hybrid Geofind–PSO algorithm. In contrast, BESS scheduling at the community level was optimised via a genetic algorithm to reduce daily costs by 20%. Simulations were performed with an hourly time step in Python, representing a static optimisation approach that does not capture short-term system dynamics. Similarly, the work in [16] introduced a linear bi-level optimisation framework for resource scheduling in ECs, explicitly targeting cost reduction under uncertainty. The results showed that integrating hydrogen resources not only enhanced flexibility but also reduced overall energy supply costs. However, simulations were conducted at an hourly time step, reflecting a static approach that overlooked the system's transient behaviour. MILP and NLP formulations were employed in [17] to approximate the upper-level objective in a bi-level optimisation framework for renewable energy communities. The model aimed to maximise shared energy and incentives at the community level while minimising costs for individual participants, demonstrating economic benefits and computational efficiency suitable for online applications.

Regarding online and real-time applications, [18] addressed the resilient operation of ECs by integrating E and solving the real-time stage with a decentralised alternating direction method of multipliers (ADMM) model to ensure robustness against worst-case demand realisations and PV uncertainty. However, the dynamic behaviour of RETs and ESSs was not considered. Despite studies such as [19], which employed a 5-min time step for real-time operation, and [20], which used a 5-s time step to handle the optimisation problem, the fast dynamics of RETs were not adequately considered. The aforementioned approaches typically adopt a static or quasi-static framework, neglecting the rapid variations inherent to power generation and consumption. Consequently, the dynamic control of prosumer-based energy communities over very short sampling times, as well as real-time power management, remains largely unexplored, despite its critical importance for ensuring system stability, operational flexibility, and rapid responsiveness under highly variable operating conditions. This gap highlights the need for advanced control strategies capable of capturing short-term variations while coordinating distributed renewable generation, storage, and demand under dynamic operation.

To address the lack of dynamic management in previous works, model predictive control (MPC) has emerged as a key technique for dynamic power allocation [21]. In [22], MPC was applied to manage a residential EC under uncertainty to reduce operational costs. The MPC controller leveraged a stochastic scenario tree to account for potential disturbances over the planning horizon, operating within a hierarchical, distributed framework. Similarly, [23] implemented a tube-based MPC to dynamically adjust energy schedules based on updated forecasts and electricity prices, maximising local renewable utilisation while

Table 1
Comparison of the proposed control with the state-of-the-art.

Paper	Time horizon	Optimisation method	RETs	BESS	Control Objective	Adaptive objectives	Multiple benchmark Comparison
18	Seconds	ADMM	X	X	Cost, Computational Time	No	Centralised, decentralised
19	5-min	ADMM	X	X	Cost	No	Two
20	5-min	Balancing-response	X	X	Cost	No	No
21	15-min	MPC	X	X	Overall benefit	No	No
22	1-h	Tree-based MPC	X	X	Cost	No	No
23	5-min	Flexible MPC	X	X	Cost, environmental	Yes	Centralised, decentralised
24	1-h	MPC	X	X	Balancing generation	No	No
25	1-h	ANN rule based	X	X	Cost, self-consumption	Yes	Rule-based
Paper	Microseconds ($50{\cdot}10^{-6}$)	Adaptive MPC	X	X	Cost, self-sufficiency, losses minimisation, RETs usage maximisation	Yes	Self-sufficiency fixed MPC, economic benefits fixed MPC, multiobjective PSO

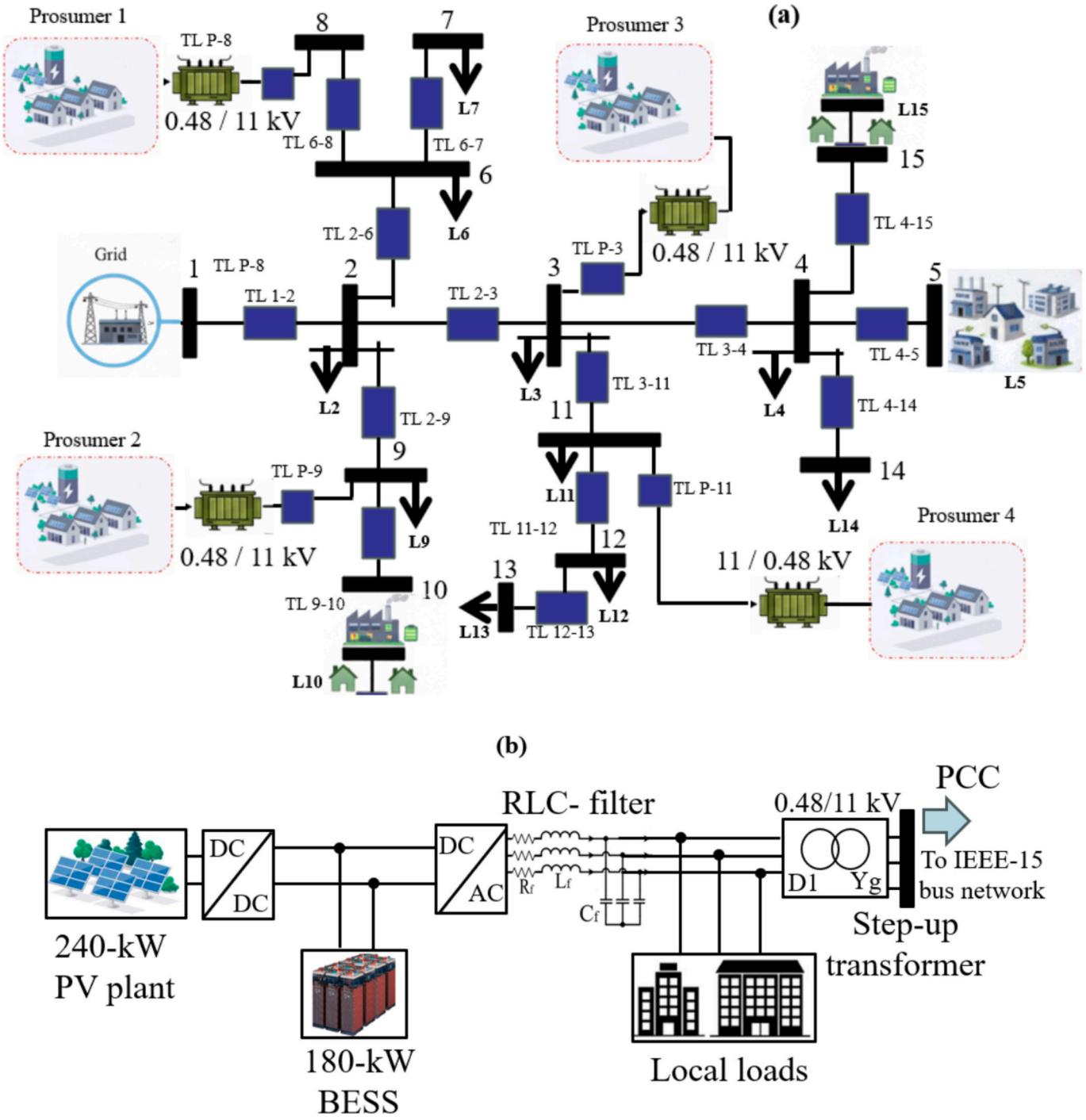

Fig. 1. Configuration of the prosumer-based EC: (a) IEEE-15 bus network EC and (b) prosumer architecture.

minimising costs. Extending this approach to interconnected communities, [24] employed a rolling-horizon MPC to coordinate local market operations and dynamic energy exchanges, exploiting short-term flexibility from storage and responsive demand. Across these studies, MPC consistently enabled communities to adapt to changing conditions, improve operational efficiency, and maintain reliable performance in both local and interconnected energy systems.

Nevertheless, adaptive predictive strategies, such as artificial neural networks (ANN) present a significant advancement over conventional MPC frameworks for the optimal management of ECs, primarily by addressing the critical challenge of model-plant mismatch in a highly dynamic environment [25]. Unlike conventional MPC, which relies on a fixed and often inaccurate system model, AMPC dynamically updates its internal predictive model using current operational data. Consequently, AMPC achieves a more precise and efficient economic dispatch by accounting for time-varying parameters, such as solar irradiance, BESS SOC or dynamic market prices, thereby minimising operational costs more effectively than its non-adaptive counterpart. Furthermore, adapting the control objective to the operating conditions leads to superior performance and enhanced system stability. Table 1 provides an overview of the existing literature.

Traditional EMS operating at day- or hour-level horizons typically optimise average power flows, under the assumption that the underlying system is stable and can instantaneously track power references.

However, this assumption breaks down in ECs with high renewable penetration and low inertia, where rapid power fluctuations must be accounted for to ensure dynamic power operation. An EMS that overlooks these fast dynamics may generate power setpoints that are economically optimal but physically infeasible. To address this challenge, this work proposes a framework that co-optimises short-term economic objectives with hardware dynamic constraints, requiring both a high-fidelity model and a sampling time on the order of microseconds.

In this work, a dynamic AMPC EMS framework is proposed for the energy management of prosumer-based ECs. The approach is specifically designed to capture the fast dynamics of RETs, ESSs, and variable loads with a sampling time of 50 microseconds, enabling the EC to adapt its operation according to dynamic market prices, available prosumer capacity, and total community demand. Unlike conventional MPC strategies, the proposed AMPC incorporates generation losses, renewable energy utilisation, and dynamic adaptation of control weights, constraints, and energy allocation. This provides comprehensive, multi-objective optimisation that ensures economic efficiency, energy sustainability, and operational flexibility.

The main **novel contributions** of this study can be summarised as follows:

1) Dynamic modelling of the EC: A detailed model of the EC is developed with a sampling time of 50 microseconds, capturing rapid variations in PV generation, BESS operation, and dynamic loads within the IEEE-15 bus network. This modelling approach provides an accurate representation of the short-term dynamics of power converters, enabling a high-fidelity dynamic framework.
2) Design of an Adaptive MPC framework for dynamic operation: The proposed AMPC optimises and adapts the EC operation based on dynamic conditions, including global operating cost, generation losses for each prosumer, and RET utilisation, enabling adaptive multi-objective optimisation. To this end, the community demand, the available prosumer capacity, and the dynamic electricity market prices are considered. Control weights, power constraints, and energy allocation are dynamically updated based on each prosumer's available capacity, ensuring efficient, flexible, and sustainable operation.
3) Complete comprehensive performance evaluation: The proposed AMPC is benchmarked against two traditional fixed-parameter MPC strategies, which focus solely on either prosumer power control or operational cost minimisation. Furthermore, the AMPC's multi-objective performance is compared against a baseline particle swarm optimisation (PSO) algorithm, demonstrating superior adaptability, operational efficiency, and effective response under highly dynamic conditions.

The remainder of this paper is organised as follows: Section II develops the dynamic model of the prosumer-based EC implemented on the IEEE 15-bus network. Section III introduces the proposed dynamic AMPC EMS. For comparison, Section IV details a multi-objective PSO algorithm that serves as a performance baseline. Subsequently, Section V presents and discusses the simulation results. Finally, Section VI draws the main conclusions from this work.

2. Dynamic modelling of prosumer-based local energy community

The dynamic modelling framework proposed in this work enables the representation of the fast dynamic behaviour of a prosumer-based EC, explicitly accounting for the rapid response of power electronic converters interfaced with RETs and ESSs, with a sampling time of 50 microseconds. Based on the consolidated IEEE-15 bus network framework, an EC comprising four prosumers was modelled and connected at different nodes together with a set of distributed passive loads. The architecture of the prosumer-based EC is illustrated in Fig. 1a.

Two prosumers with a rated capacity of 420 kW were considered, each comprising a 240 kW PV plant, a 180 kW BESS, and local loads. Additionally, two prosumers with a rated capacity of 360 kW were modelled, each including a 180 kW PV power plant, a 180 kW BESS, and associated local loads. The operation within each prosumer was managed by a DC/DC converter that maintained the PV plant at its maximum power point (MPPT) based on the available solar irradiance at each instant. The outputs of the BESS and the PV plant were connected to a common DC bus.

Furthermore, a three-phase DC/AC converter operating in grid-following mode controlled the power each prosumer injected into the energy community. To this end, a phase-locked loop (PLL) measured grid voltage and current, while a conventional PWM control coordinated the power delivered by each prosumer. An RLC filter was installed to smooth the output of the DC/AC converter, and a step-up transformer adjusted the three-phase voltage from 0.48 kV to the 11 kV level of the IEEE-15 bus network. Transmission lines connecting prosumers, consumers, and the primary grid were modelled as short RL lines, and the external grid was represented as a real three-phase voltage source. The structure of each prosumer is shown in Fig. 1b.

The non-linear dynamic model for a PV cell is given by:

$$I_{PV} = I_{ph} - I_o \left[e^{\left(\frac{V_{PV} + I_{PV} R_s}{n V_T} \right)} - 1 \right] - \frac{V_{PV} + I_{PV} R_s}{R_{sh}} \tag{1}$$

where I_{PV}does the panel generate the current, V_{PV} is the panel voltage, I_{ph} is the photocurrent proportional to irradiance, I_o is the reverse saturation current of the diode, and R_s and R_{sh} are the series and shunt (or parallel) resistances, respectively.

The BESS was modelled using the SimPowerSystems Toolbox in Simulink. Its mathematical description considered parameters such as the open-circuit voltage (V_{BESS}), terminal current (I_{BESS}), internal resistance (R_{int}), nominal capacity (Q_{BESS}), and initial state of charge (SOC_O). The resulting dynamic model was expressed through the following equations:

$$V_{BESS} = E_{BESS} - I_{BESS} \cdot R_{int} \tag{2}$$

$$SOC(\%) = SOC_O(\%) - 100 \left(\frac{\int I_{BESS} \cdot dt}{Q_{BESS}} \right) \tag{3}$$

3. Adaptive model predictive control

This section details the design of a novel AMPC EMS proposed in this paper for the optimal dynamic coordination of prosumers within the EC described in Section 2. The proposed control architecture is based on a two-level approach. First, the low-level local control is described, which is responsible for the instantaneous power management of RETs and ESSs, ensuring the safe operation within the technical limits of each prosumer.

Subsequently, the AMPC is presented in-depth as the high-level, centralised coordinator. The primary contribution of this work lies in the multiobjective optimisation within dynamic adaptive weights. This function simultaneously seeks to: (i) maximise the coverage of community demand with prosumers' resources, (ii) minimise the total operational cost of the EC, (iii) minimise generation power losses within each prosumer and primary grid, and (iv) maximise the utilisation of available renewable generation (i.e., self-consumption). The adaptive mechanism autonomously adjusts the priority of these objectives (the cost function weights) based on the electricity market price signal, enabling the community to transition between different operational strategies intelligently. Finally, the adaptive nature of the AMPC is complemented by the inclusion of dynamic operational constraints that adjust the optimiser's decision boundaries based on the available dynamic power capacity from the assets.

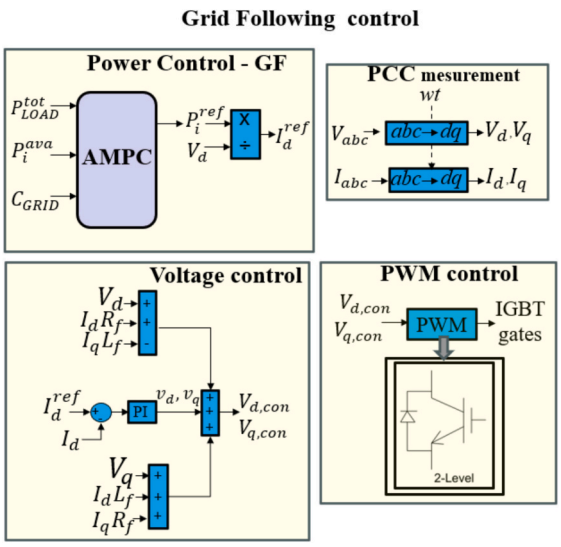

Fig. 2. Prosumer power converter control.

$$V_{d,con} = V_d + I_d R_f - I_q L_f + v_{d,i} \tag{4}$$

$$V_{q,con} = V_d + I_d L_f + I_q R_f + v_{q,i} \tag{5}$$

3.1. Low-level local control

First-level control is centred on managing the power injection from every prosumer. Within the specific configuration of the EC, a grid-following inverter governs the local power dispatch, as depicted in Fig. 2. Achieving exact synchronisation with the AC voltage at the point of common coupling (PCC) is critical for these inverters to ensure proper voltage and frequency control. This task is managed by a phase-locked loop (PLL). This framework implements a power-based control scheme that forgoes traditional frequency and voltage droop methods. In this approach, the active power setpoints are designated for each prosumer, $P_{n,k}^{ref}$, are used to calculate the necessary current references, I_d^{ref} and I_q^{ref}, by normalising them with the direct voltage component, V_d. The subsequent control layer manages the direct and quadrature current components, (I_d, I_q), to ensure they precisely track their setpoints. Any deviation is corrected by a PI-based current regulator, which produces the control signals $v_{d,i}$ and $v_{q,i}$ to command the inverter's voltage. To counteract the inherent coupling between the direct and quadrature axes, a feedforward decoupling mechanism is implemented as described in eqs. (4) and (5). The final stage utilises a PWM modulator to create the necessary switching signals for the inverter.where R_f and L_f denote the resistance and inductance values of the inverter's output filter.

3.2. Adaptive multiobjective predictive control for optimal local energy community management

The dynamic coordination of an EC presents a complex control challenge, characterised by variable generation/demand profiles and a set of inherently conflicting operational objectives. Traditional MPC approaches, while effective for constrained systems, typically rely on a static cost function, rendering them suboptimal in the face of dynamically changing operational priorities and market conditions [26]. To overcome this limitation, this paper proposes a novel AMPC framework to manage the power flows of $N = 4$ prosumers intelligently.

The core innovation of the proposed AMPC lies in its ability to dynamically arbitrate among competing objectives by adjusting the control policy based on the model's current state. This paradigm shift enables the EC to operate in two modes, prioritising either EC self-sufficiency or economic efficiency. The primary variable governing the economic strategy is the dynamic electricity purchasing price from the primary grid. This allows the controller to select its operational focus intelligently:

- First, when the grid import tariff exceeds the internal cost of dispatching energy from prosumers, the AMPC strategy assigns greater weight to the demand coverage objective. The controller's primary goal is to minimise the error between the total EC demand and the power delivered by the prosumers. Moreover, this strategy enables achieving the highest possible level of energy self-sufficiency, thereby insulating the EC from expensive market conditions.
- Conversely, suppose the grid price is lower than the dispatch cost from one or more prosumers. In that case, the AMPC strategy shifts its priority by assigning a dominant weight to the minimisation of operational costs. In this opportunistic mode, the controller leverages the favourable market condition by importing cheaper energy from the grid to cover a portion of the demand. At the same time, the most cost-effective local prosumers supply the remaining load. Moreover, this strategy reduces power losses associated with each prosumer's generation by curtailing the contributions of the more expensive prosumers, thereby lowering those losses.

3.2.1. System modelling and predictive formulation

The proposed AMPC is architected as a multivariable control system designed to regulate the key performance indicators of the energy community. The control structure is defined by four manipulated variables (MVs), which constitute the control input vector u_k, and four measured outputs (MOs), which form the output vector y_k The controller aims to drive the system towards a desired reference trajectory. Fig. 3a represents the AMPC dynamic weighting, and its configuration scheme is depicted in Fig. 3b.The manipulated variables are the reference power setpoints for each of the $N = 4$ prosumers within the community $\left(P_{i,k}^{ref}\right)$. The control vector at each discrete time step k is therefore defined as:

$$u_k = \begin{pmatrix} P_{1,k}^{ref} \\ P_{2,k}^{ref} \\ P_{3,k}^{ref} \\ P_{4,k}^{ref} \end{pmatrix} \tag{6}$$

The AMPC's optimisation algorithm computes these setpoints based on predictions of EC operating states, including local demand, renewable energy availability, and grid electricity prices.

The output vector quantifies the system's response y_k, which comprises four critical performance metrics: the total power dispatched by the prosumers ($P_{P,k}^{tot}$), the total instantaneous operating cost ($C_{op,k}^{tot}$), the total generation power losses ($P_{loss,k}^{tot}$), and a renewable energy utilisation index ($U_{f,k}$). This vector is expressed as:

$$y_k = \begin{pmatrix} P_{P,k}^{tot} \\ C_{op,k}^{tot} \\ P_{loss,k}^{tot} \\ U_{f,k} \end{pmatrix} \tag{7}$$

The total prosumer power $\left(P_{P,k}^{tot}\right)$ is defined as the algebraic sum of the power dispatched by all prosumers:

$$P_{P,k}^{tot} = \sum_{i=1}^{N} P_{i,k} \tag{8}$$

where P_i denotes the power of each prosumer.

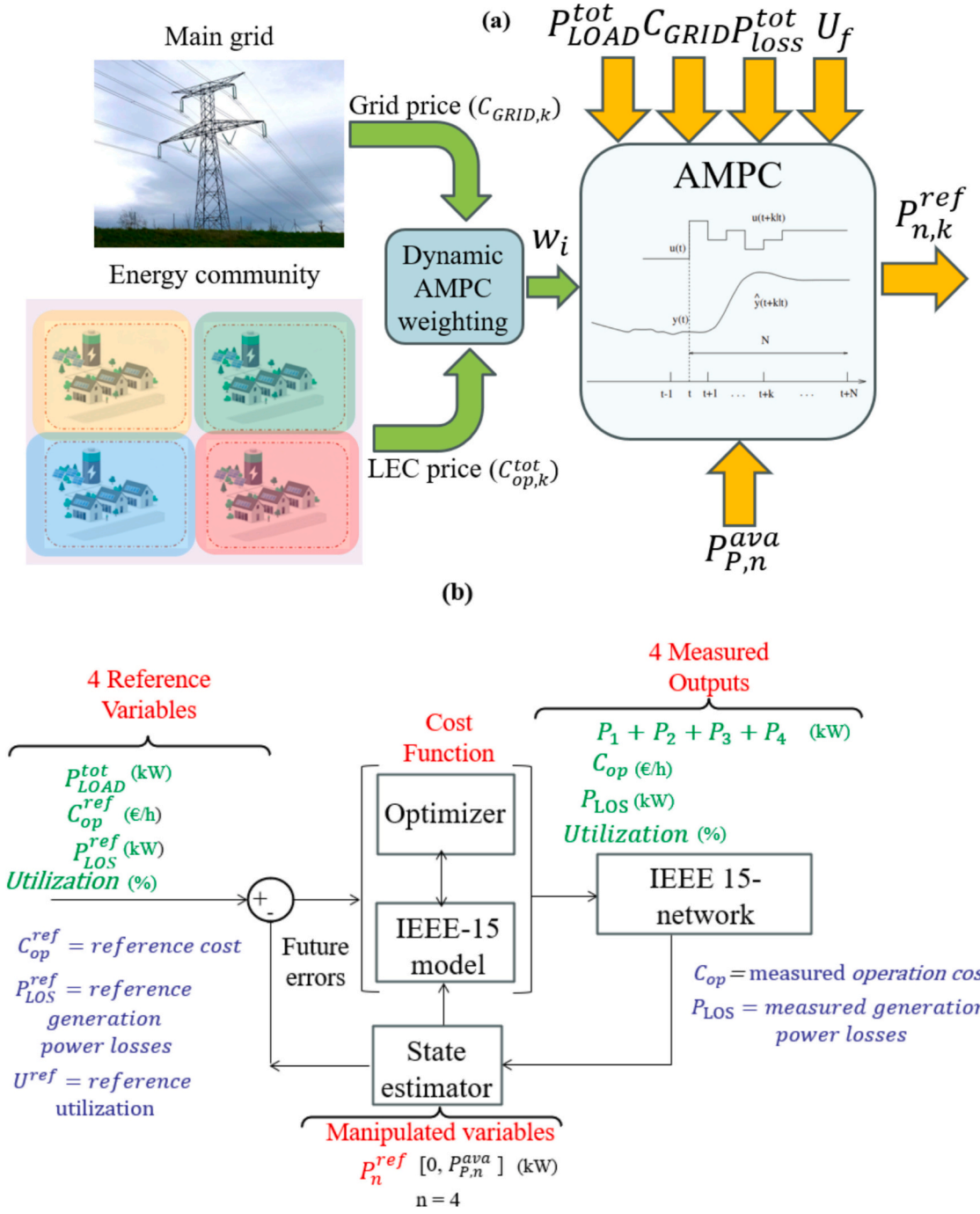

Fig. 3. (a) Dynamic AMPC weighting and (b) AMPC configuration scheme.

The total cost $\left(C^{tot}_{op,k}\right)$ considers the energy cost of each prosumer, the cost of energy purchased from the primary grid, and the cost associated with power losses:

$$C^{tot}_{op,k} = \sum_{i=1}^{N} P_{i,k} \cdot C_{P,i,k} + P_{GRID,k} \cdot C_{GRID,k} + P^{tot}_{loss,k} \cdot C_{LOSS,k} \tag{9}$$

where $P_{GRID,k}$ is the power delivered from the primary grid, $P^{tot}_{loss,k}$ is the total power losses, $C_{P,i,k}$ is the individual energy cost of each prosumer, $C_{GRID,k}$ is the main grid energy price and $C_{LOSS,k}$ is the cost of energy losses cost.

The total power losses $\left(P^{tot}_{loss,k}\right)$ aggregates the generation losses, modelled as a function of the currents flowing from each prosumer and the grid:

$$P^{tot}_{loss,k} = \sum_{j=1}^{N+1} R_j \cdot I^2_{j,k} \tag{10}$$

where R_j denotes the equivalent resistance of each prosumer and the grid transmission line, and $I_{j,k}$ Is the current flowing from each prosumer or from the primary grid?

The RETs utilisation factor $\left(U_{f,k}\right)$ is an index designed to measure the effective use of the available capacity according to:

Table 2
AMPC parameters.

Item	Parameter	Value
Controller parameters	T_s Sample time (s)	0.01
	P_H Prediction horizon (s)	100
	C_H Control horizon (s)	10
Constraints MV	P_{P1}^{ref} (kW)	[0, P_1^{ava}]
	P_{P2}^{ref}(kW)	[0, P_2^{ava}]
	P_{P3}^{ref} (kW)	[0, P_3^{ava}]
	P_{P4}^{ref}(kW)	[0, P_4^{ava}]
Constraints MO	P_{LOAD}^{tot} (kW)	–
	C (€/h)	[0, ∞]
	P_{loss}^{tot} (kW)	[0, ∞]
	U_f (%)	[0,1]
Weights MO	$P_{P,k}^{tot}$ (kW)	10 (high priority) – 0.1 (low priority)
	C (€/h)	10 (high priority) – 0.1 (low priority)
	P_{loss}^{tot} (kW)	1 – medium priority
	U_f (%)	1 – medium priority

$$U_{f,k} = \sum_{i=1}^{N} \frac{P_{i,k} \cdot P_{i,k}^{ava}}{\left(P_{i,k}^{ava}\right)^2} \tag{11}$$

where $P_{i,k}^{ava}$ is the dynamic available power of each prosumer.

The control objective is to steer the output vector y_k towards a reference vector r_k, defined as:

$$r_k = \begin{pmatrix} P_{LOAD,k}^{tot} \\ C_{op,k}^{ref} \\ P_{loss,k}^{ref} \\ U_{f,k}^{ref} \end{pmatrix} \tag{12}$$

where $P_{LOAD,k}^{tot}$The total EC demand is the sum of the loads connected to the nodes of the IEEE-15 bus network. For the other objectives, ideal references are established to guide the optimisation: the reference cost ($C_{op,k}^{ref}$) and reference losses ($P_{loss,k}^{ref}$) are set to zero, while the ideal utilisation reference ($U_{f,k}^{ref}$) is set to one. Although these ideal setpoints for cost and losses are physically unattainable due to the demand constraint, they establish a clear optimisation direction. The AMPC's core task is thus to minimise the deviation from this reference trajectory while rigorously adhering to the system's operational constraints.

Table 2 represents the parameters employed in the design of the AMPC. The recommendations outlined in [27] were followed to define the high-, medium-, and low-priority weights.

3.2.2. Dynamic multiobjective optimisation problem

At each time step k, the AMPC solves a constrained, finite-horizon optimisation problem. The goal is to compute an optimal sequence of future control actions, U, which contains the manipulated variable setpoints over a defined control horizon, C_H. This optimisation is performed over a prediction horizon, P_H. The optimisation problem seeks to find the control sequence U that minimises a comprehensive cost function, J, which aggregates the performance objectives over the prediction horizon. The formulation is as follows:

$$\min J(x_k, U) = \sum_{i=k}^{k+P_H-1} w_{i,k} \cdot J_{i,k} \tag{13}$$

where for each time step k within the prediction horizon, w_i is the column vector of adaptive weights and J_i is the column vector of the objective functions. These are explicitly defined as:

$$w_{i,k} = \begin{pmatrix} w_{LOAD,k} \\ w_{cost,k} \\ w_{LOSS,k} \\ w_{U,k} \end{pmatrix} \quad J_{i,k} = \begin{pmatrix} J_{LOAD,k} \\ J_{COSt,k} \\ J_{LOSS,k} \\ J_{U,k} \end{pmatrix} \tag{14}$$

where the term $J_{LOAD,k}$ represents the error between $P_{LOAD,k}^{tot}$ and $P_{P,k}^{tot}$; $J_{COSt,k}$, the error between $C_{op,k}^{ref}$and $C_{op,k}^{tot}$; $J_{LOSS,k}$, the error between $P_{loss,k}^{ref}$ and $P_{loss,k}^{tot}$; and finally, $J_{U,k}$, the error between $U_{f,k}^{ref}$and $U_{f,k}$.

Physically, the first term ($J_{LOAD,k}$) acts as the primary control lever for community self-sufficiency. Given that the grid exchange is inherently defined as the residual of the load-generation balance (see Eq. (15)), there exists a direct structural equivalence: minimising the tracking error is mathematically identical to minimising grid dependency. Consequently, assigning a high priority to this objective reshapes the optimisation landscape, compelling the AMPC to treat the load-generation match as the dominant target. This actively suppresses external imports and forces the prosumers to dispatch their maximum available power to bridge the gap. Therefore, it increases each prosumer's self-sufficiency and the utilisation of their available power. In contrast, under scenarios where grid interaction is economically permitted (reduced weighting assigned to $w_{LOAD,k}$), the reliance on internal assets is alleviated, as the primary grid participates in the demand coverage. Therefore, this shift reduces the operational stress on prosumers, naturally leading to a lower utilisation factor of the installed renewable capacity.

The optimisation is subject to the following fixed and dynamic constraints for all $i \in [k, k + P_H - 1]$.First, the power balance constraint must be satisfied at every time step, which is formulated as:

$$\sum_{i=1}^{N} P_{i,k} + P_{GRID,k} = P_{LOAD,k}^{tot} + \sum_{j=1}^{N+1} R_j \cdot I_{j,k}^2 \tag{15}$$

Furthermore, a key novelty of the proposed AMPC is the incorporation of dynamic constraints based on the available capacity of each prosumer. This formulation represents a fundamental advancement over the standard constraint handling found in recent literature, where operational limits are typically treated as static, decoupled parameters.

For instance, recent studies, such as [28,29], rely on fixed thresholds for SOC (SOC_{min}, SOC_{max}) and constant power saturation limits (P_{min}, P_{max}), ignoring the dynamic reduction of battery capability near its physical limits. Similarly, [30] employs static energy boundaries (E_{min}, E_{max}) and restricts PV generation based on a fixed performance rate, a simplification that fails to account for efficiency drops due to surface temperature variations. Furthermore, approaches such as [31] utilise static state-of-energy (SOE) limits while treating renewable generation as a separate, decoupled variable.

A common limitation across these approaches is that none integrates the stochastic nature of generation and the state-dependent storage capability into a unified parameter. In contrast, the proposed framework introduces a unified dynamic availability metric. This approach aggregates the varying PV irradiance, the instantaneous SOC-dependent battery capability, and the local load demand into a single, time-varying term. This creates a dynamic feasibility envelope that updates at every sampling instant, ensuring that the optimisation is constrained by the prosumer's actual, real-time physical inertia. Consequently, the dynamic available power is formulated as:

$$P_{i,k} \leq P_{i,k}^{ava} \tag{16}$$

where the term $P_{i,k}^{ava}$ is expressed as:

$$P_{i,k}^{ava} = P_{PV,i} + P_{BESS,i} - P_{P,LOAD,i} \tag{17}$$

where $P_{PV,i}$ denotes the power from the PV array, $P_{BESS,i}$ is the power dispatched by the BESS, and $P_{P,LOAD,i}$ is the prosumer's consumption. The value of $P_{PV,i}$ is directly dependent on dynamic solar irradiance.

Additionally, to ensure the BESS operation within safe and effective limits [32], dynamic constraints on its state of charge (SOC) are defined according to:

$$P^{max}_{BESS,dis} = min\left(P^{rated}_{BESS}, \frac{E^{nom}_{BESS}}{\Delta t}.\left(\frac{SOC - SOC_{min}}{100}\right)\right) \quad (18)$$

$$P^{max}_{BESS,ch} = min\left(P^{rated}_{BESS}, \frac{E^{nom}_{BESS}}{\Delta t}.\left(\frac{SOC_{max} - SOC}{100}\right)\right) \quad (19)$$

where $P^{max}_{BESS,dis}$ denotes the peak discharge power, and $P^{max}_{BESS,ch}$ specifies the maximum charging capacity of the BESS, while P^{rated}_{BESS} defines its nominal power. The variable $\frac{E^{nom}_{BESS}}{\Delta t}$ corresponds to the rate of energy change within the BESS, whereas SOC_{min} and SOC_{max} define the lowest and highest permissible states of charge for the battery, respectively.

3.2.3. Adaptive MPC weighting strategy

The central contribution of this work lies in the intelligent mechanism that governs the adaptive priority weight vector, $w(k)$. Unlike conventional MPC approaches that rely on static priorities or predefined scheduling, the proposed framework employs a state-aware supervisory logic to reconfigure control objectives dynamically.

Crucially, the modulation of $w(k)$ operates through a strictly autonomous, event-driven architecture, where control transitions are triggered instantaneously by operating changes. The logic continuously monitors the instantaneous grid electricity price, C_{GRID}, acting as an exogenous state variable. The supervisor evaluates the market condition against the prosumer internal unitary generation cost ($C_{P,i,k}$), which serves as the economic break-even threshold. The adaptive mechanism is mathematically formulated as:

$$w(k) = \begin{cases} w_{LOAD,k} = 10 \text{ and } w_{cost,k} = 1 \text{ if } C_{GRID} > C_{P,i,k} \\ w_{cost,k} = 10 \text{ and } w_{LOAD,k} = 1 \text{ if} C_{P,i,k} > C_{GRID} \end{cases} \quad (20)$$

This formulation ensures that the controller's adaptation is responsive to dynamic market volatility. It reflects the fundamental premise that the strategic value of operational objectives is not constant but context-dependent. When $C_{GRID} > C_{P,i,k}$, the pursuit of economic efficiency physically converges with self-sufficiency; and thus, the supervisor actively reconfigures the cost function topology to prioritise demand coverage ($w_{LOAD,k} = 10$, $w_{cost,k} = 1$) preventing the AMPC from drifting towards grid imports. Conversely, when favourable market conditions arise ($C_{GRID} < C_{P,i,k}$), the logic reverts to economic optimisation ($w_{LOAD,k} = 1$, $w_{cost,k} = 10$), exploiting the price differential.

Consequently, the primary driver for this adaptation is the dynamic relationship between external prices and internal costs, which dictates the transition between two distinct operational modes:

Self-Sufficiency Mode: During periods when the grid electricity price is high and purchasing external energy becomes economically prohibitive, the framework activates a self-sufficiency mode. In this scenario, the AMPC's logic shields the community from the expensive market by assigning a high-priority weight to the demand-coverage objective, $w_{LOAD,k}$ while significantly reducing the importance of the cost objective $\left(w_{LOAD,k} \text{"} w_{cost,k}\right)$. The controller's overriding goal becomes to operate as an autonomous entity, minimising the power imported from the grid. It is crucial to highlight that, in this context, the pursuit of self-sufficiency implicitly aligns with the minimum-cost operation, as utilising internal resources is physically the most cost-effective strategy. However, by explicitly prioritising the demand coverage weight, the controller structurally enforces the ECs self-sufficiency, preventing the AMPC from drifting towards expensive grid imports.

Economic optimisation mode: Conversely, when market conditions are favourable and the grid price is low, the controller switches to economic optimisation mode. This situation presents a clear opportunity to reduce operational expenditures. The priorities shift decisively, and the weight for the cost objective, $w_{cost,k}$, is given dominant importance ($w_{cost,k}$ " $w_{LOAD,k}$). The AMPC then seeks the most economically efficient power dispatch, typically resulting in a hybrid solution in which part of the demand is served by the cheapest prosumers and the remainder is imported opportunistically from the low-cost grid. This economically driven strategy naturally minimises generation losses as prosumers are less stressed. The undesirable, yet accepted, consequence is a reduction in the utilisation factor of the community's own renewable assets in favour of the immediate economic benefit.

The weights for loss minimisation ($w_{LOSS,k}$) and available capacity maximisation ($w_{U,k}$) remain fixed across both operational modes. They are assigned as a medium priority, reflecting their status as secondary objectives that are consistently desirable. Their role is to ensure underlying technical efficiency and system resilience, regardless of whether the controller's primary focus is on a purely prosumer-based operation or on maximising economic benefit.

The dynamic arbitration between these two modes is the cornerstone of the contribution. It represents a significant advancement over conventional methods. Regarding the rationale for this strategy, it stems from the fundamental limitation that a conventional MPC with fixed weights is forced into a “perpetual, suboptimal compromise”. Such a rigid configuration becomes suboptimal the moment external conditions change, rendering it incapable of either fully exploiting low-cost market opportunities or adequately shielding the community from price spikes.

During low-price periods, for example, a static controller fails to capture significant economic surplus by unnecessarily restricting grid imports. Conversely, during high-priced periods, it erodes economic value by failing to enforce self-sufficiency fully. The proposed adaptive weighting is therefore necessary because it provides the critical flexibility to dynamically decouple and prioritise conflicting control objectives in response to real-time operating conditions—specifically, the grid electricity price. In a fluctuating market, the relative strategic value of ‘minimising operational cost’ versus ‘maximising self-sufficiency’ is not constant; it is context-dependent. By dynamically modulating the weights ($w_{cost,k}$, $w_{LOAD,k}$), the framework actively reshapes the cost function's topology to reflect this shifting reality. This ensures that the optimiser strictly aligns its primary control goal with the immediate economic context, effectively prioritising the requisite level of self-sufficiency over secondary technical constraints when market conditions dictate the need for autonomy.

This capacity for dynamic strategy adaptation—allowing the controller to reconfigure its objectives while satisfying variable operational constraints—is the essential feature that distinguishes this framework. It marks a paradigm shift from a fixed, compromise-based methodology to a dynamic, truly optimal control strategy, a transition essential for enabling the economic and resilient operation of modern energy systems.

4. Multiobjective particle swarm optimisation benchmark

To rigorously evaluate the performance of the proposed AMPC framework, a benchmark optimisation strategy is established based on the PSO algorithm. PSO is a well-regarded metaheuristic technique, celebrated for its efficacy and robustness in navigating complex, nonlinear search spaces without requiring gradient information [33]. Its established success in solving power dispatch problems makes it an ideal candidate for a comparative baseline.

The multiobjective problem—minimising power control error, minimising costs, minimising losses, and maximising RET utilisation—is adapted for the PSO algorithm by aggregating these four objectives into a single composite fitness function. This is achieved through a weighted-sum approach, where each objective is assigned a weight (w_P,w_C,w_L,w_U) that reflects its relative importance. To ensure a balanced optimisation, a uniform weighting factor of 0.25 is allocated to each control objective. In this case, w_P denotes the weighting factor that minimises the error between the EC demand and the delivered power from the prosumers

Table 3
PSO algorithm sequence.

Step	Procedure
1	Define objective function: M.O.F = minEq.(13) Define the vector of power trajectories:
2	$x = \left[P^{ref}_{P1,k}, P^{ref}_{P2,k}, P^{ref}_{P3,k}, P^{ref}_{P4,k}\right]$ with bounds $P_{i,k} \leq P^{ava}_{i,k}$ $i = 1,,,,N$
3	The initial step involves creating a population of M particles $x_i \in \mathbb{R}^N$, where each particle's position serves as a candidate solution. Every particle is also initialised with a velocity vector, v_i
4	For every particle in the swarm, the fitness value is computed using the objective function described in Eq. (13). Based on this evaluation, the personal and global best solutions are then updated
5	The velocity and position of every particle are then revised using the following expression: $v(k+1) = w \cdot v^k + r_1 c_1 (x_{pbest}{}^k - x^k) + r_2 c_2 (g_{pbest}{}^k - x^k)$ In these equations, w represents the inertia weight, c_1 and c_2 are the acceleration coefficients, while r_1 and r_2 are random numbers uniformly distributed in the range (0,1).
6	The algorithm iteratively executes steps 4 and 5 until convergence is achieved. This occurs when either the predefined maximum number of iterations is reached or the improvement in the fitness function becomes insignificant.
7	The optimal solution, $x^* = g$, is identified as the one that produces the minimum value for the objective function defined in Eq. (13).

and the primary grid. Moreover, w_C and w_L are the weighting factors to minimise the overall costs and the power generation losses. Finally, w_U denotes the weighting factor that maximises the utilisation of available power for each prosumer. The decision variables for the optimisation are the power setpoints of the $N = 4$ prosumers, represented by the particle's position vector $x = [P^{ref}_{P1,k}, P^{ref}_{P2,k}, P^{ref}_{P3,k}, P^{ref}_{P4,k}]$. The multiobjective function to be solved is the same as described in Eq. (13).

The PSO algorithm deploys a population of particles, each representing a potential solution (x), and iteratively updates their velocity and position based on their own best-known solution (p_{best}) and the global best-known solution (g_{best}) found by the entire swarm [34]. The particle dynamics are governed by the following procedure, described in Table 3:

5. Results and discussion

This section presents a comprehensive analysis of the proposed AMPC's performance in a dynamic control and optimisation approach, considering the transient states of renewable generation, energy storage, variable loads and dynamic grid energy price. To this end, section 5.2 presents results obtained with the proposed AMPC controller, demonstrating its ability to adapt the EC's operation to dynamic operational variations optimally. Section 5.3 provides a comparison with a traditional MPC where the control objective emphasises meeting demand exclusively by using the prosumers within the EC. Section 5.4 offers another comparison using a traditional MPC, this time with the control objective focused on the continuous economic optimisation of the EC. Moreover, Section 5.5 compares the AMPC with the PSO algorithm described in section 4, which serves as a recognised benchmark. Finally, Section 5.6 provides a final benchmark against an adaptative PSO.

5.1. Sensitivity analysis for time step selection

The numerical validation of the proposed AMPC framework was executed within the MATLAB/Simulink environment (version R2022a). The computational testbed consisted of a workstation equipped with an AMD Ryzen 77,700 8-core processor operating at 4.50 GHz, 64 GB of RAM, and Windows 11 Enterprise. Regarding the solver configuration, a discrete fixed-step approach was adopted with a temporal resolution of

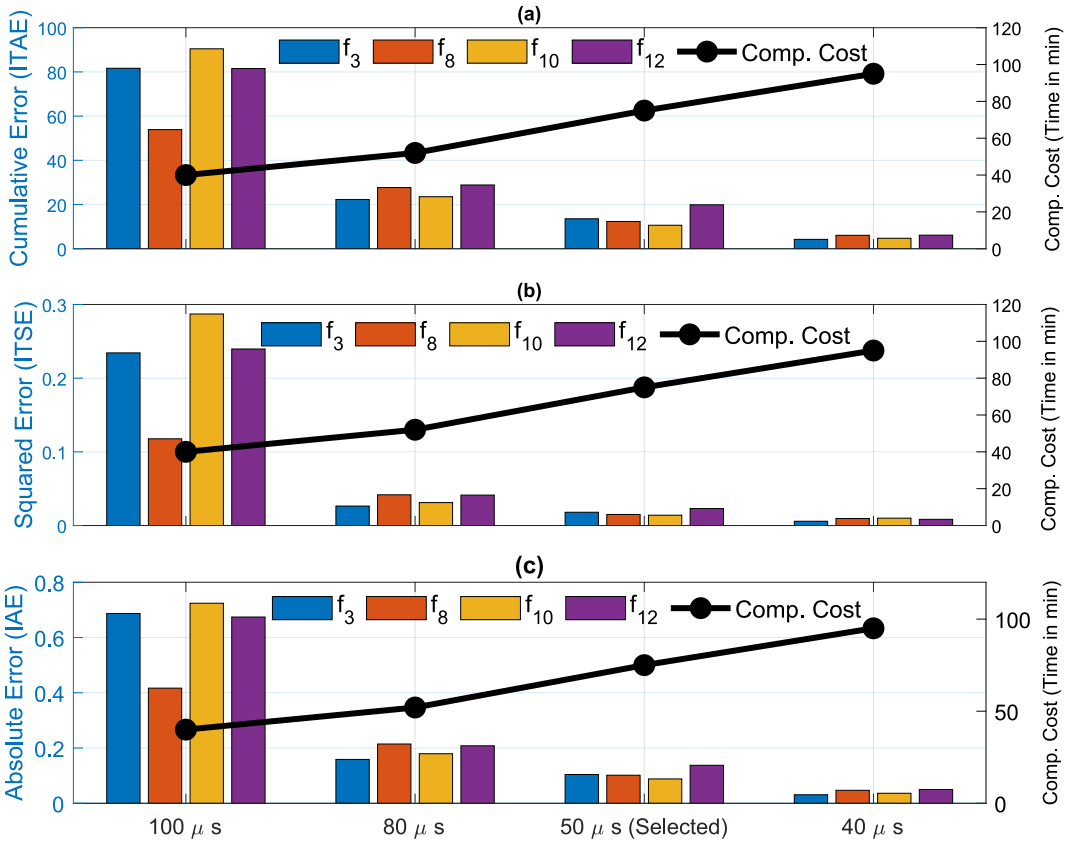

Fig. 4. Sensitivity analysis: Computational cost vs. frequency control fidelity (f_1, f_2, f_3 and f_4) across varying time steps.

Table 4
EC parameters.

Symbol	Parameter	Unit
V_{nom}	Rated voltage	11 kV
f_{nom}	Rated frequency	60 Hz
L_{1-2}	Line parameters per phase	1.351 Ω + 3.517 mH
L_{2-3}	Line parameters per phase	1.1702 Ω + 3.036 mH
L_{2-6}	Line parameters per phase	2.557 Ω + 4.575 mH
L_{2-9}	Line parameters per phase	2.013 Ω + 3.602 mH
L_{3-4}	Line parameters per phase	0.841 Ω + 2.182 mH
L_{3-11}	Line parameters per phase	1.796 Ω + 3.213 mH
L_{4-5}	Line parameters per phase	1.532 Ω + 2.726 mH
L_{4-14}	Line parameters per phase	2.231 Ω + 3.991 mH
L_{4-15}	Line parameters per phase	1.197 Ω + 2.142 mH
L_{6-7}	Line parameters per phase	1.088 Ω + 1.947 mH
L_{6-8}	Line parameters per phase	1.251 Ω + 2.239 mH
L_{9-10}	Line parameters per phase	1.687 Ω + 3.018 mH
L_{11-12}	Line parameters per phase	2.448 Ω + 4.381 mH
L_{12-13}	Line parameters per phase	2.013 Ω + 3.602 mH
L_f	Filter inductance	1.08 mH
R_f	Filter resistance	1.08 mΩ
C	Filter capacitance	184 μF
m	Step-up transform voltage relationship	0.48 / 11 kV

50 μs.

To rigorously justify the selection of the simulation time step, a sensitivity analysis was conducted to quantify the trade-off between optimisation costs and control fidelity. While EC load profiles typically exhibit slow temporal variations, the stability of a low-inertia, converter-dominated prosumers is fundamentally governed by the fast-switching dynamics of the power electronics. Therefore, relying on coarse time steps suitable for steady-state dispatch risks masking critical voltage and frequency transients.

To address this, the study evaluates the response of the four frequency control signals (f_1, f_2, f_3 and f_4) under four resolution scenarios (100, 80, 50, 40 μs). The quantitative analysis begins with Fig. 4a, which presents the ITAE (integral time absolute error). At coarser resolutions (80–100 μs), the data reveals a critical tracking failure. Specifically, at 100 μs, the ITAE for the signal f_3 peaks at 90.45, while the ITAE for f_4 is equal to 81.51. Even reducing the step to 80 μs results in elevated errors (ITAE for f_4 is equal to 28.84), confirming that high time steps fail to capture the controller's dynamics. This inadequacy is quantified strictly in Fig. 4b using the ITSE (integral time squared error), which penalises large transients. At 100 μs, the ITSE reaches unacceptable values across the spectrum (ITSE for f_3 is equal to 0.287; ITSE for f_4 is equal to 0.240). These magnitudes indicate significant oscillatory behaviour and

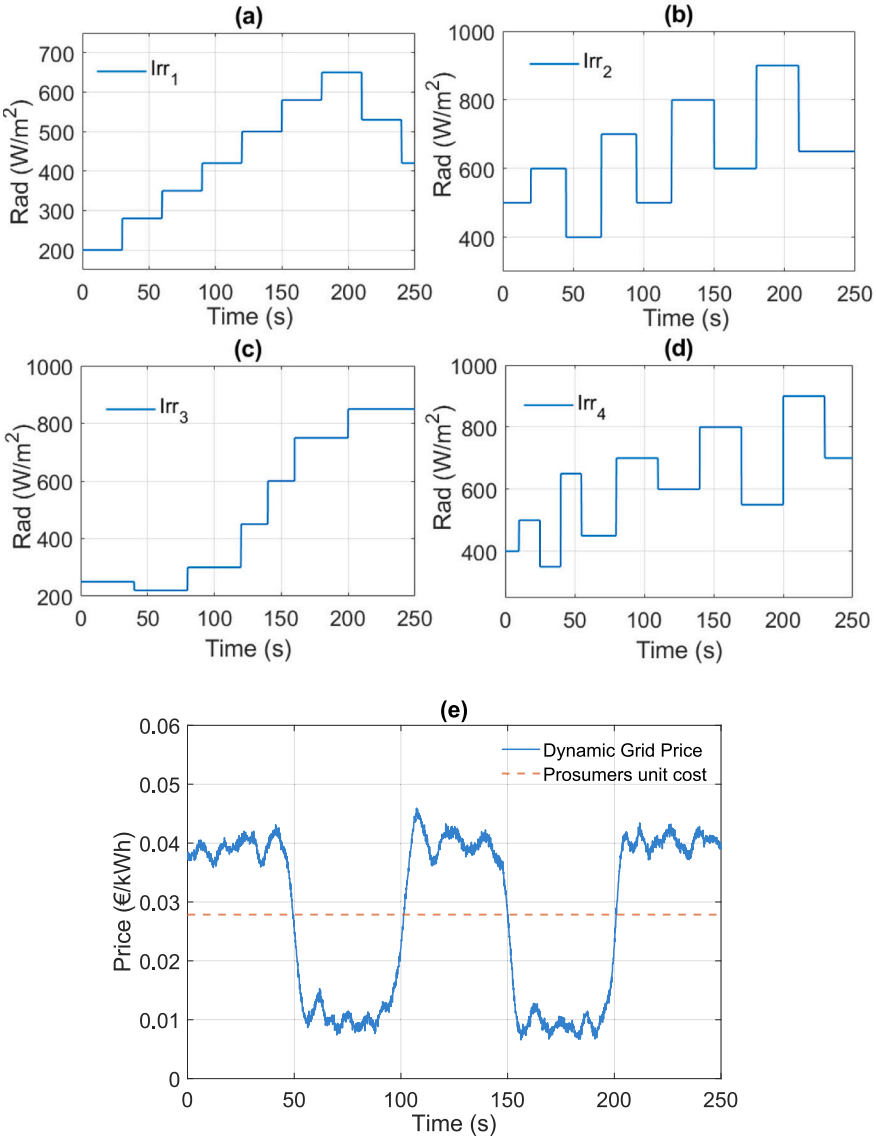

Fig. 5. Irradiation profiles and primary grid energy price: (a) *Prosumer*$_1$, (b) *Prosumer*$_2$, (c) *Prosumer*$_3$ (d) *Prosumer*$_4$ and (d) primary grid price.

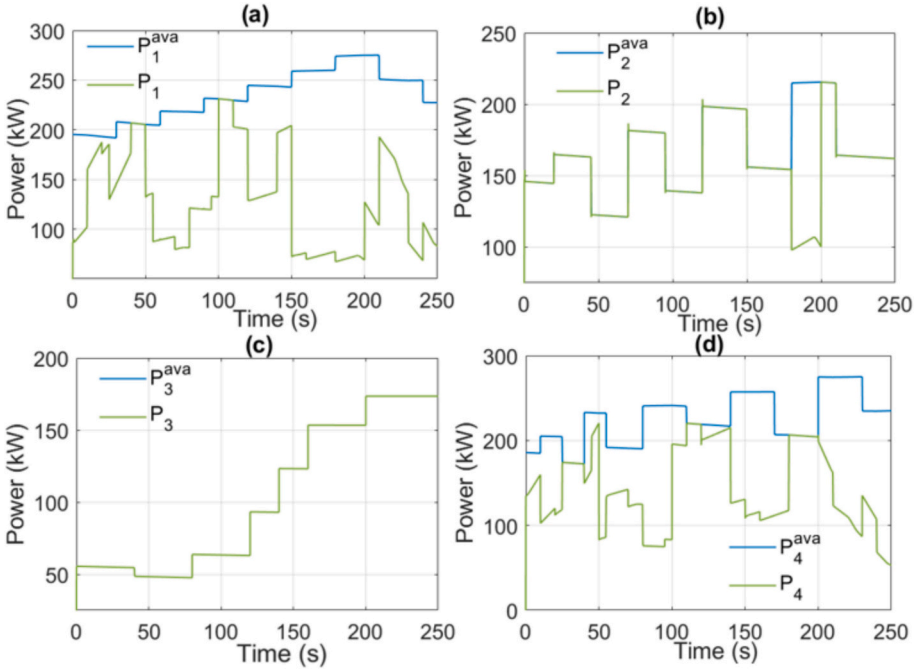

Fig. 6. Prosumer capacity and delivered power: (a) Prosumer$_1$: P_1^{ava} and P_1, (b) Prosumer$_2$: P_{P2}^{ava} and P_2, (c) Prosumer$_3$: P_3^{ava} and P_3 and (d) Prosumer$_4$: P_4^{ava} and P_4.

numerical instability. Although these coarse scenarios offer a normalised computational cost of 40 min, the high ITSE values render these results physically invalid for stability analysis.

In contrast, the transition to 50 μs marks the definitive convergence point where physical validity is restored. As evidenced in Fig. 4a, the ITAE for f_3 drops from 90.45 to 10.63, representing an 88% reduction in cumulative error. More critically for system safety, Fig. 4b shows that the ITSE collapses by an order of magnitude, stabilising at 0.014 for f_3 and 0.023 for f_{12}. This numerical evidence confirms that at 50 μs, the large oscillatory transients are effectively eliminated, ensuring robust frequency regulation. While this resolution increases the simulation time to the reference baseline (75 min), this cost is necessary to model the inverters' inner-loop dynamics accurately.

Finally, the analysis rules out the need for higher resolutions based on diminishing returns observed in the integral absolute error (IAE), as depicted in Fig. 4c. Reducing the time step further to 40 μs increases the computational burden by 27% (reaching 95 min). However, the performance gain is negligible in practical terms: the ITSE for the total power (f_{12}) only decreases from 0.023 to 0.008. Given that the system is already stable at 50 μs, paying a 27% higher computational penalty for this marginal refinement is inefficient. Consequently, 50 μs is selected as the optimal operating point, balancing high-fidelity representation with rational computational costs.

5.2. Adaptive MPC dynamic performance

The effectiveness of the proposed control strategy is validated in this section through simulations involving variable solar irradiance, EC demand, and grid energy prices. The operational parameters for the considered EC, illustrated in Fig. 1, are provided in Table 4.

Fig. 5 depicts the irradiance profile and the primary grid price used in a detailed 250-s simulation. For clarity, the subscript 'i' is used to denote variables corresponding to each prosumer, such as their individual irradiance, PV power, BESS power, and power delivered to the EC. A very short time step of 50 μs was selected to ensure an accurate representation of the EC's dynamic behaviour. This high-resolution time step enables a high-fidelity model of the power electronics, accounting for the switching dynamics of each prosumer's DC/DC and DC/AC converters. Such a detailed representation is a critical aspect often neglected in conventional EC and prosumer integration studies.

Fig. 6 illustrates the distribution of P_i^{ava} and P_i for each prosumer. The proposed AMPC is designed to ensure an optimal power allocation from economic, efficiency, and sustainability perspectives. One of the control objectives is to keep the dispatched power from each prosumer as close as possible to the available power, thereby maximising the utilisation of RETs.

This goal, however, creates an inherent trade-off: minimising generation losses can increase system losses, and vice versa. The AMPC framework effectively resolves this conflict by predictively optimising each prosumer's operating point and dynamically adapting to the primary grid's energy price.

During the initial simulation phase (0–50 s), the main grid energy price exceeds the prosumers' internal generation costs. Consequently, the AMPC adapts its control policy to satisfy the EC demand using exclusively local prosumers, thereby avoiding the high cost of grid-imported energy. For instance, at t = 20s, the EC demand is set to 492 kW. The available power from each prosumer is P_1^{ava}=208 kW, P_2^{ava}=145 kW, P_3^{ava}=55 kW, and P_4^{ava}=205 kW. To meet the demand, the AMPC dispatches 174 kW from P_1, 145 kW from P_2, 55 kW from P_3, and 118 kW from P_4.

At t = 50s, a transient event occurs, representing variations in irradiance across the EC. This results in a shift in available power: P_1^{ava}=increases to 250 kW, P_2^{ava} decreases to 121 kW, P_3^{ava} drops to 48 kW, and P_4^{ava}rises to 232 kW. In response, the AMPC immediately recalculates the optimal dispatch, assigning P_1=205 kW, P_2=121 kW, P_3 =48 kW, and P_4=217 kW, successfully meeting the new total demand of 591 kW and demonstrating its rapid adaptability regarding the demand and the current power capability.

In the subsequent interval (50–100 s), a new scenario is introduced where the grid electricity price falls below the prosumers' internal dispatch cost. This triggers the AMPC to switch to its economic optimisation mode, where the control objective shifts to minimising total operational costs by allowing energy procurement from the grid. At t = 75 s, the EC demand ranges between 600 and 650 kW, and the primary grid contributes nearly 200 kW to meet this load. At this instant, the available power from each prosumer is P_1^{ava}=218 kW, P_2^{ava}=181 kW, P_3^{ava}=64 kW, and P_4^{ava}=190 kW.

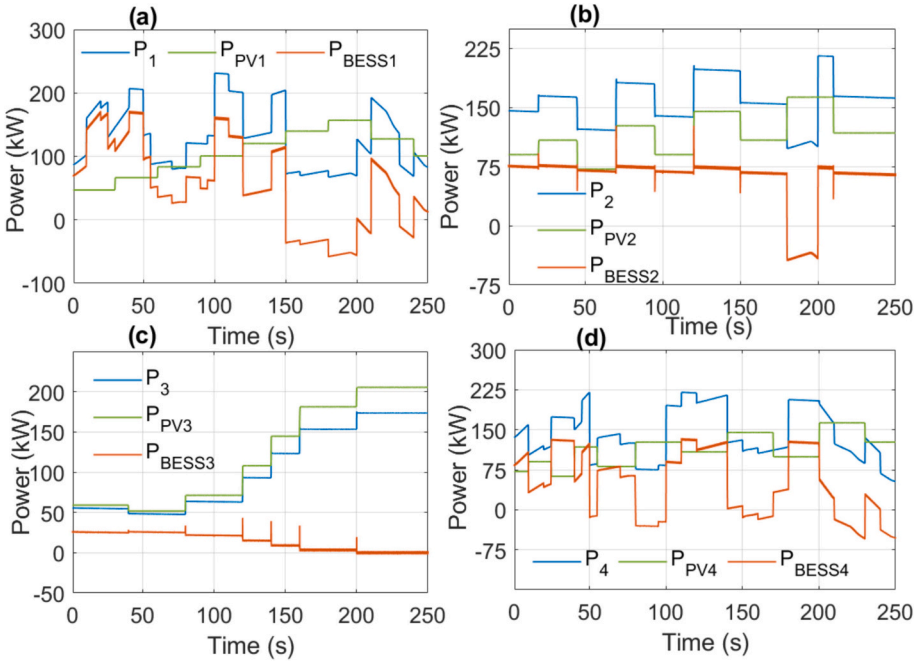

Fig. 7. AMPC prosumer internal power: (a) Prosumer$_1$: P_1, $P_{PV,1}$, $P_{BESS,1}$ (b) Prosumer$_2$: P_2, $P_{PV,2}$, $P_{BESS,2}$, (c) Prosumer$_3$: P_3, $P_{PV,3}$, $P_{BESS,3}$ and (d) Prosumer$_4$: P_4, $P_{PV,4}$, $P_{BESS,4}$.

Consequently, the prosumers are only required to supply the remaining two-thirds of the demand, leading to a beneficial reduction in generation losses but also to lower utilisation of available capacity. The AMPC resolves this by dispatching 81 kW from P_1, 181 kW from P_2, 63 kW from P_3, and 124 kW from P_4 to complete the power balance. This distribution ensures absolute cost minimisation, deliberately sacrificing higher RET utilisation for economic gain. The remainder of Fig. 6 continues to demonstrate the AMPC's seamless transitions between these high- and low-price operational modes.

Fig. 7 provides a detailed breakdown of the internal power dispatch for each prosumer, illustrating the individual contributions from the PV system ($P_{PV,i}$) and the BESS ($P_{BESS,i}$) to meet both the dispatched power command (P_i) and the local load. In the initial high-price scenario, the controller prioritises self-sufficiency. For prosumer 1 (Fig. 7a), it has dispatched 174 kW, and the local load of 25 kW is met by a combined 46 kW from its PV system and 153 kW from its BESS. Similarly, prosumer 2's (Fig. 7b) total contribution of 145 kW to the EC and its 15-kW local demand is supplied by 85 kW of PV generation and 75 kW from its BESS. The power balance for prosumer 3 (Fig. 7c) consists of 60 kW from the PV array and 20 kW from the BESS to cover a 55-kW dispatch and a 25-kW load. Finally, prosumer 4 (Fig. 7d) meets its 118 kW EC commitment and 15 kW local consumption using 90 kW of PV power and 43 kW from its BESS.

Conversely, during the low-price period (50–100 s), the strategy shifts to economic optimisation, and the prosumers' dispatch power is adjusted accordingly. For prosumer 1, the dispatched 81 kW and its 25-kW load are satisfied by 83 kW from the PV system and only 23 kW from the BESS, highlighting a notable reduction in BESS contribution. To meet the 181 kW required by prosumer 2 and its 15 kW local load, the PV system delivers 127 kW. In comparison, the BESS provides the remaining 69 kW, again reducing its dispatch compared to the previous scenario. In the case of prosumer 3, it has been assigned 63 kW, and the 25 kW local load is met by 71 kW from the PV power plant and 17 kW from the BESS. Lastly, the 124-kW command for prosumer 4 and its 15-kW local demand are supplied by 81 kW of PV generation and 58 kW from the BESS.

Furthermore, the results demonstrate the local management of surplus energy. In scenarios where PV generation exceeds the sum of the local load and the dispatched power command, the excess energy is injected into the BESS. This behaviour, which prevents renewable energy curtailment, can be observed for prosumer 1 between 150 s and 200 s (Fig. 7a) and for prosumer 4 after 200 s (Fig. 7d).

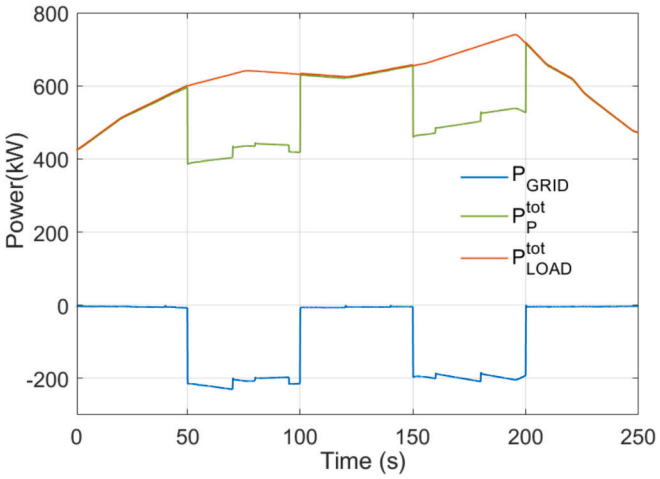

Fig. 8. EC power control involves prosumers, the grid, and dynamic loads.

Fig. 8 provides a compelling validation of the AMPC's dynamic arbitration capabilities, illustrating the dynamic power distribution between the prosumer collective ($P^{tot}_{P,k}$) and the primary grid (P_{GRID}) to meet the total EC demand (P^{tot}_{LOAD}). The results showcase a series of instantaneous and strategic shifts in control philosophy, driven by external market signals. In the initial phase (0–50 s), confronted with high grid energy prices, the AMPC's control logic correctly prioritises self-sufficiency. It forces the EC into a fully autonomous, grid-independent mode, compelling $P^{tot}_{P,k}$ to precisely track the 400–600 kW demand while P_{GRID} is held at zero.

A stark and immediate strategic transition occurs at $t = 50$s when the grid price becomes economically favourable against the prosumer's operation. The AMPC detects this opportunity and seamlessly pivots to

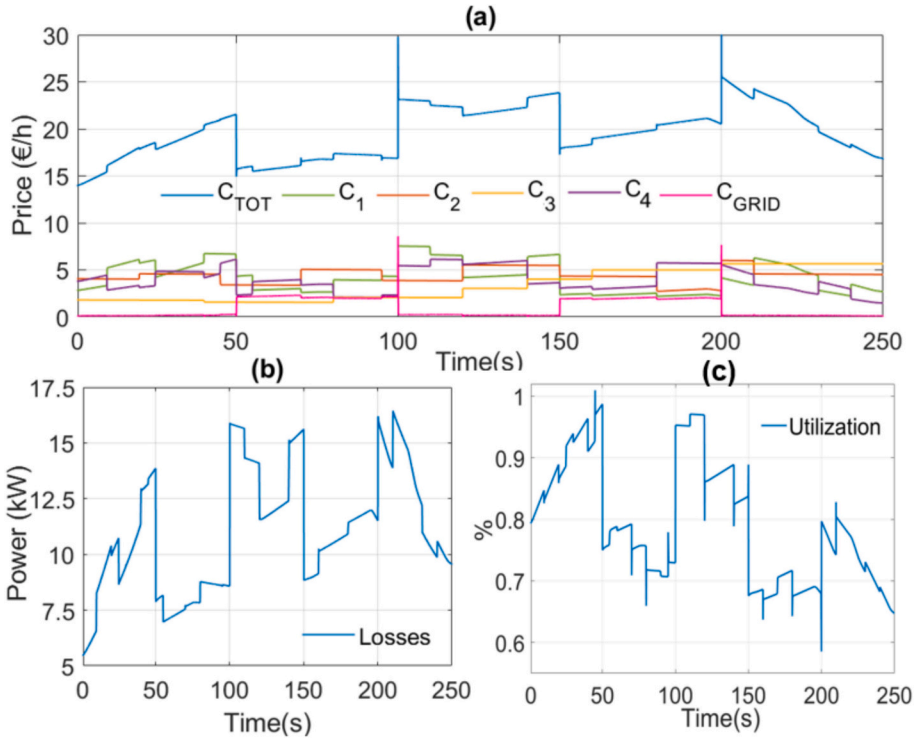

Fig. 9. AMPC control objectives: (a) total cost, (b) generation power losses and (c) utilisation factor.

its economic optimisation mode. In this state (50–100 s), the grid is dispatched to supply a stable 200 kW, while the prosumer contribution is modulated to meet the remaining 400–450 kW of demand. This demonstrates a sophisticated co-optimisation: the controller not only imports cheap energy but also simultaneously adjusts the prosumer dispatch to minimise generation losses, striking an intelligent balance that avoids the complete abandonment of RETs.

The subsequent intervals further challenge the controller, proving its robustness under more demanding conditions. Between 100 s and 150 s, the grid price rises again, and despite a higher demand profile (630–655 kW), the prosumers once more demonstrate their capacity to achieve full autonomy, curtailing grid power to zero. This response is critical, as relying on the high-priced grid under such loads would render the operation economically unviable. The final periods (150–250 s) showcase the AMPC's agility in managing rapid, successive transitions. The controller first re-engages the grid to optimise costs as demand peaks towards 740 kW. Then, upon a final price spike at $t = 200$ s, it once again avoids purchasing energy from the grid, perfectly tracking a steep, decreasing demand transient without any external support. This confirms the controller's ability to not only make optimal steady-state decisions but also to manage transient conditions with precision and stability.

Fig. 9 provides a conclusive validation of the AMPC's performance by deconstructing its impact on the three primary optimisation objectives: total cost (Fig. 9a), total generation losses (Fig. 9b), and the RETs utilisation factor (Fig. 9c). The results reveal a sophisticated and continuous arbitration between these competing goals, orchestrated dynamically by the adaptive controller.

The economic performance, depicted in Fig. 9a, is particularly insightful in highlighting the benefits of the proposed AMPC. The AMPC achieves an impressively low average operational cost of 19.58 €/h for the EC. The figure vividly illustrates the controller's two distinct economic philosophies. During high-price intervals (e.g., 0–50 s), the grid's cost contribution is driven to zero, as the AMPC enforces an autonomous operational mode to shield the community from the high market prices. Conversely, during low-price periods (e.g., 50–100 s), the controller seizes the economic opportunity by importing 200 kW from the grid, as it is cheaper than the dispatch cost of prosumers 1, 2, and 4. The controller's intelligence is further highlighted by its handling of prosumer 3. It dispatches this prosumer at its maximum available capacity (63 kW) precisely because it recognises this as an optimal decision that simultaneously yields low cost, low associated generation losses, and full utilisation of that particular asset.

The interplay between efficiency and autonomy is clearly visible in the analysis of system losses and RET utilisation. As shown in Fig. 9b, total generation losses are inherently higher during the self-sufficiency modes (e.g., 0–50 s, 100–150 s, 200–250 s) when the prosumers are heavily dispatched. However, when the AMPC transitions to economic optimisation (e.g., 50–100 s, 150–200 s), relying on the grid reduces prosumer effort, leading to a corresponding and beneficial drop in losses. The controller maintains an average power loss of only 11.02 kW, demonstrating its effective management of system efficiency. Inversely, the RET utilisation factor is illustrated in Fig. 9c. The utilisation factor logically peaks during self-sufficiency operation when local prosumers are paramount. Conversely, it is deliberately reduced when the AMPC identifies an economic advantage in procuring cheaper grid power. The resulting average utilisation of 79.31% is a testament to the framework's balanced approach, confirming its ability to integrate renewables effectively while still capitalising on market opportunities.

These results demonstrate that the proposed AMPC performs as an intelligent economic and technical dispatcher. It successfully navigates the complex trade-offs among cost, efficiency, and sustainability, proving its suitability for ensuring a power dispatch that is simultaneously economically viable and highly efficient, while guaranteeing a profound integration of renewable energy resources. The following sections provide a detailed comparison with the introduced AMPC, a fixed-MPC strategy, and a PSO algorithm.

5.3. Comparison against the self-sufficiency fixed MPC

To quantify the tangible benefits of the proposed adaptive strategy, a comparative analysis is performed against a conventional self-

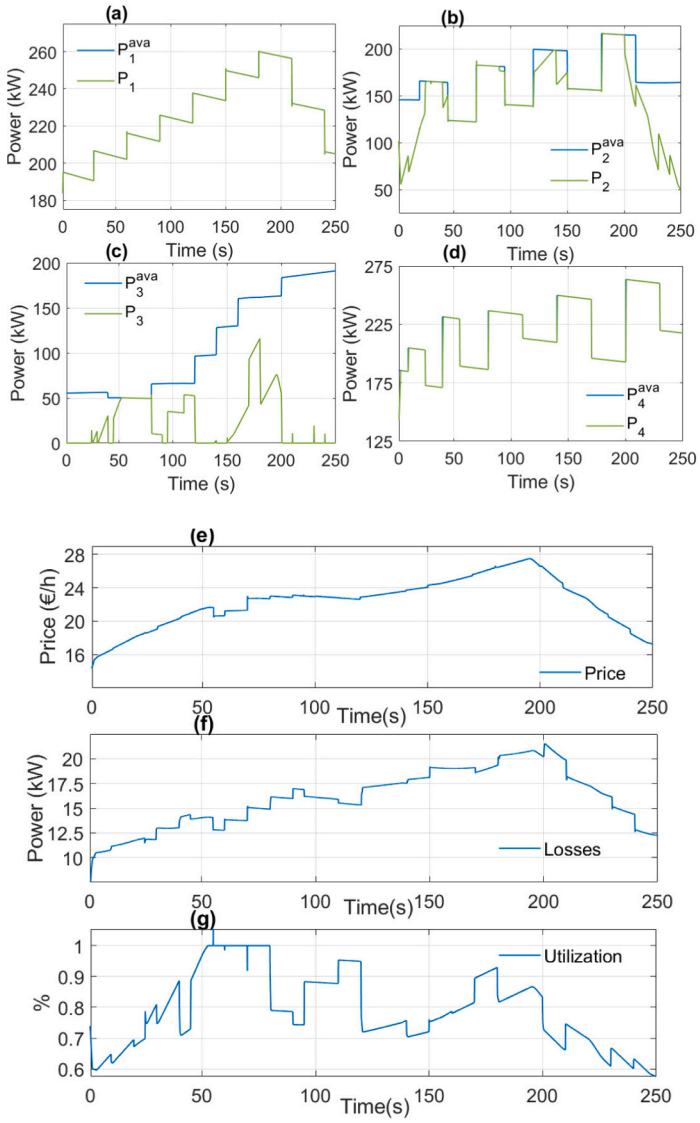

Fig. 10. Self-sufficiency MPC results: (a) Prosumer$_1$: P_1^{ava} and P_1, (b) Prosumer$_2$: P_2^{ava} and P_2, (c) Prosumer$_3$: P_3^{ava} and P_3, (d) Prosumer$_4$: P_4^{ava} and P_4, (e) total costs, (f) power losses and (g) utilisation factor.

sufficiency MPC (SS-MPC). This benchmark controller utilises the same predictive framework as the AMPC but employs a fixed set of weights that consistently prioritise maximising the EC's autonomy. By design, the SS-MPC represents a standard, non-adaptive approach, providing a stark baseline against which the intelligence of the AMPC can be measured. The subsequent analysis subjects both controllers to the identical operational scenarios presented in Section 5.1.

Fig. 10 reveals the inherent rigidity and critical weaknesses of the static SS-MPC approach. During the initial high-price period (0–50 s), the SS-MPC successfully meets the 492-kW demand. Specifically, it dispatches 190 kW from prosumer 1 (Fig. 10a), 137 kW from prosumer 2 (Fig. 10b), and 165 kW from prosumer 4 (Fig. 10d). In comparison, prosumer 3 is set at 0 kW (Fig. 10c). This dispatch reveals the controller's decision-making logic, prioritising units with the highest available capacity. The controller's flaw is exposed at $t = 50$s, when the grid price drops. Blind to this crucial economic signal, the SS-MPC continues to enforce its rigid self-sufficiency policy.

It forces the prosumers to meet the entire 600–650 kW demand, dispatching high power levels (213 kW for prosumer 1, 187 kW for prosumer 2, 60 kW for prosumer 3 and 190 kW for prosumer 4) and completely ignoring the opportunity to procure low-cost energy from the grid.

This strategic failure has severe economic and technical consequences. In the 75 s, the SS-MPC's stubborn autonomy resulted in an instantaneous cost of 22.68 €/h and generation losses of 15 kW. In stark contrast, under the same conditions, the AMPC's intelligent pivot to its economic optimisation mode yields an instantaneous cost of just 17.19 €/h and losses of only 7.8 kW. This represents a staggering 31.94% reduction in cost and a 92% reduction in losses, a direct result of the AMPC's ability to adapt. While the SS-MPC controller achieves 100% RET utilisation during this interval, it incurs an unjustifiable economic and efficiency penalty compared to the AMPC's balanced 75.7% utilisation.

Extrapolating this analysis over the entire simulation confirms the profound superiority of the adaptive approach. The SS-MPC yields a high average operational cost of 22.3 €/h, which is 13.89% more expensive than the AMPC's average of 19.58 €/h, as depicted in Fig. 10e. Furthermore, the SS-MPC controller's inefficient dispatch results in average power losses of 15.97 kW (Fig. 10f) —a massive 44.92% higher than the 11.02 kW achieved by the AMPC. Interestingly, the average RET utilisation is almost identical, with the AMPC (79.31%) even slightly outperforming the SS-MPC (78.95%), Fig. 10g. This final result is perhaps the most damning for the SS-MPC approach: it proves that the AMPC's intelligent, adaptive strategy achieves notable lower costs and

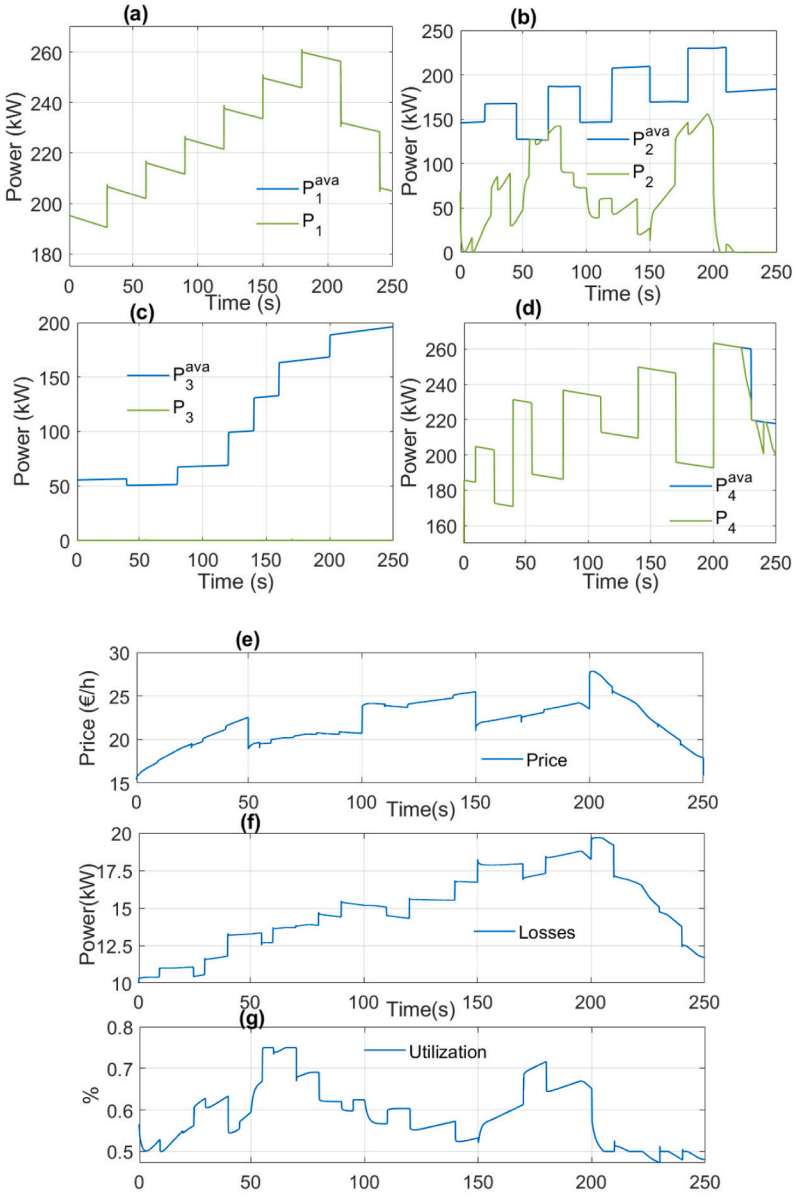

Fig. 11. Economic benefits MPC results: (a) Prosumer$_1$: P_1^{ava} and P_1, (b) Prosumer$_2$: P_2^{ava} and P_2, (c) Prosumer$_3$: P_3^{ava} and P_3, (d) Prosumer$_4$: P_4^{ava} and P_4, (e) total costs, (f) power losses and (g) utilisation factor.

losses without any meaningful sacrifice in the overall utilisation of renewable resources, solidifying its position as a truly superior control strategy.

5.4. Comparison against economic benefits fixed MPC

To complete the comparative analysis, a second benchmark, the economic benefit MPC (EB-MPC), is used. This controller represents the antithesis of the SS-MPC, as its fixed-weighting scheme consistently prioritises total cost minimisation above all other objectives. By treating the primary grid as just another dispatchable agent to be included in the economic optimisation, the EB-MPC allows for a comprehensive evaluation of the proposed AMPC against both extremes of fixed-priority control.

The results, presented in Fig. 11, immediately expose the critical vulnerability of this purely economic strategy. During the initial high-price period (0–50 s), the EB-MPC's rigid focus on a perceived cost optimum compels it to import 89 kW of expensive energy from the primary grid, while dispatching 190 kW from prosumer 1 (Fig. 11a), 48 kW from prosumer 2 (Fig. 11b), and 165 kW from prosumer 4 (Fig. 11d), leaving prosumer 3 entirely unused (Fig. 11c). While the EB-MPC behaves as expected during the low-price scenario (50–100 s) by increasing its grid reliance to 106 kW, dispatching 213 kW from prosumer 1, 141 kW from prosumer 2, and 190 kW from prosumer 4 to complete the power balance, its inability to adapt to high prices reveals a fundamental flaw.

A direct, instantaneous comparison at $t = 75$ s reveals the outcome of these three distinct control strategies. In terms of cost, the AMPC achieves a value of 17.19 €/h, significantly outperforming both the EB-MPC (20.60 €/h) and the SS-MPC (22.68 €/h)—a 19.84% cost reduction over the EB-MPC benchmark. Regarding efficiency, the AMPC again demonstrates its superiority with a power loss value of only 7.8 kW, a remarkable 77.94% improvement over the EB-MPC's 13.88 kW. Finally, in terms of RETs utilisation, the EB-MPC logically scores the lowest value at 68.98%, as the prosumers' contribution is curtailed. In contrast, the AMPC maintains a robust 75.7%, demonstrating a 9.87% enhancement in RETs usage even in a scenario where cost is a key driver.

When extrapolated over the entire simulation, the results demonstrate the effectiveness of the proposed approach. The EB-MPC yields an

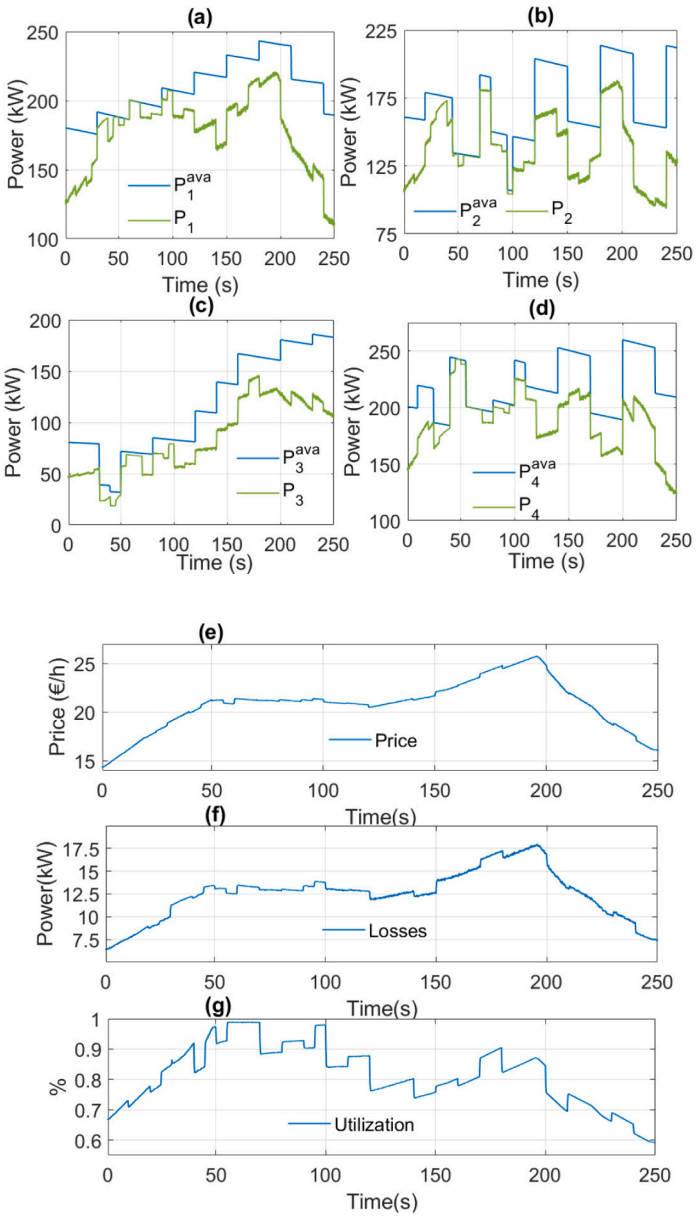

Fig. 12. Multiobjective PSO optimisation: (a) Prosumer$_1$: P_1^{ava} and P_1, (b) Prosumer$_2$: P_2^{ava} and P_2, (c) Prosumer$_3$: P_3^{ava} and P_3, (d) Prosumer$_4$: P_4^{ava} and P_4, (e) total costs, (f) power losses and (g) utilisation factor.

average operational cost of 21.99 €/h (Fig. 11e), indicating the AMPC is 12.31% more cost-effective. In terms of average losses, the EB-MPC's 14.93 kW (Fig. 11f) is 35.48% higher than the AMPC's remarkably low 11.02 kW. Most remarkably, in the metric of sustainability, the AMPC's average RET utilisation of 79.31% represents a 13.34% improvement over the EB-MPC's 68.73% (Fig. 11g). These findings show that the AMPC achieves a superior outcome in both economic efficiency and renewable energy integration compared to the controller designed purely for economic benefit.

While the EB-MPC improves costs and losses compared to the blindly autonomous SS-MPC, both fixed-priority strategies are inherently sub-optimal. The proposed AMPC demonstrates a profoundly superior performance, consistently finding an operating point that robustly balances all objectives. It does not merely compromise; it leverages its predictive and adaptive capabilities to achieve a synergistically superior outcome, proving its status as an intelligent framework for the economic, efficient, and sustainable management of modern energy communities.

5.5. Comparison against multiobjective PSO optimisation

To further demonstrate the superiority of the AMPC, its performance is compared with that of a multiobjective PSO (PSO-EMS) as formulated in Section 4. By benchmarking against a well-known metaheuristic algorithm, this analysis aims to demonstrate the unique superiority of the AMPC's predictive and adaptive capabilities over even advanced, non-predictive optimisation methods.

The results of the PSO-EMS are presented in Fig. 12. During the high-price period (0–50 s), the PSO effectively achieved a high grade of self-sufficiency, dispatching 143 kW, 142 kW, 47 kW, and 160 kW from the four prosumers, respectively. Similarly, in the low-price scenario that follows, the algorithm recalculates the dispatch, assigning 207 kW to prosumer 1, 104 kW to prosumer 2, 79 kW to prosumer 3, and 200 kW to prosumer 4. However, the PSO's decision-making, which optimises for the present instant without foresight, leads to quantifiable inefficiencies.

At $t = 75$ s, the PSO-EMS yields an operating cost of 21.17 €/h and generation losses of 13.02 kW. Compared to the AMPC's performance

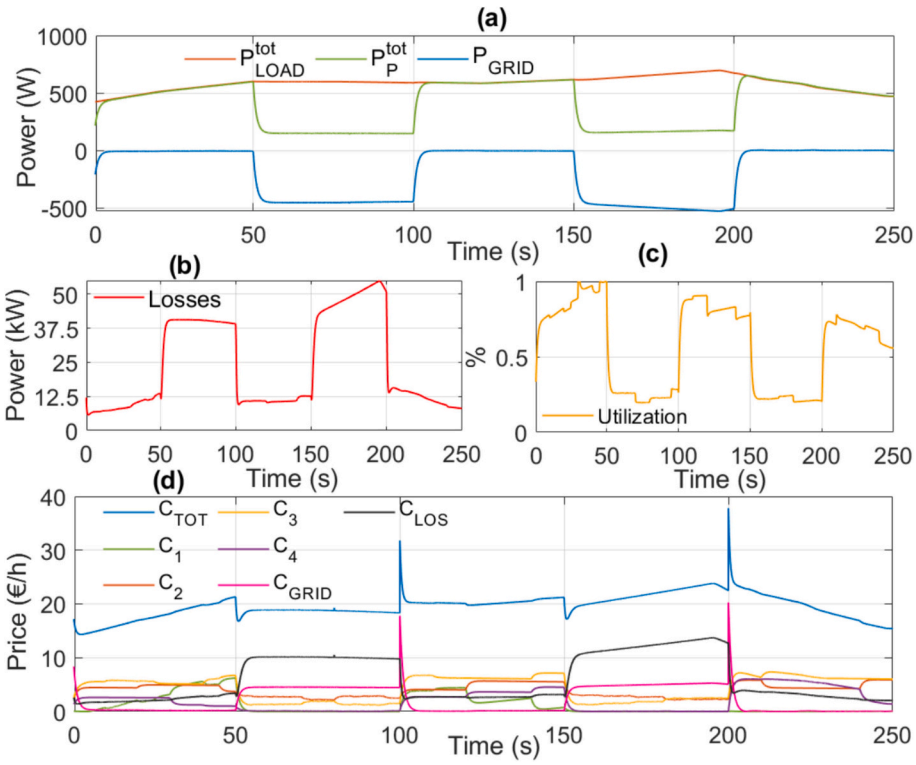

Fig. 13. Adaptive PSO optimisation: (a) power control: $P^{tot}_{\mathrm{LOAD}}, P^{tot}_{\mathrm{P}}$ and P_{GRID}, (b) power losses (c) utilisation factor and (d) cost terms: C_{TOT}, $C_1, C_2, C_3, C_4, C_{\mathrm{GRID}}, C_{\mathrm{LOS}}$

under identical conditions, this represents a 23.21% increase in cost and a 66.92% increase in losses.

This highlights a fundamental trade-off that the PSO struggles to manage optimally. The PSO's strategy results in a very high instantaneous RET utilisation of 88.85% (a 17.3% increase over the AMPC at that moment). However, this aggressive pursuit of RET maximisation comes at a steep and immediate price. The data empirically proves that a higher instantaneous RET dispatch, particularly when cheaper grid energy is available, directly correlates with significantly higher operational costs and greater power generation losses. When analysed over the entire simulation, the global results solidify the AMPC's superiority. The PSO-EMS achieves an average cost of 20.78 €/h and average losses of 12.54 kW (Fig. 12e-f), which are 6.13% and 13.79% higher than the AMPC's values, respectively. In return for these higher costs and losses, the PSO only achieves a marginal 2.53% increase in average RET utilisation (81.32%) compared to the AMPC's 79.31% (Fig. 12g).

The results demonstrate that while maximising RET utilisation is a primary goal, pursuing it aggressively without predictive foresight, as the PSO does, leads to a financially and technically inefficient outcome. The proposed AMPC, by contrast, proves its superiority regarding the dynamic power dispatch problem. The controller uses its predictions to continuously compare the cost of internal generation against the dynamic price of grid energy. This allows it to balance its objectives skilfully, ensuring a high level of RET integration while simultaneously delivering superior economic and efficiency outcomes. The exhaustive analysis presented confirms that the adaptive and predictive nature of the proposed AMPC provides a demonstrably more robust, efficient, and economically viable solution than even sophisticated, state-of-the-art static optimisation techniques like PSO and traditional MPC.

5.6. Comparison against adaptive weighting PSO strategy

In addition to the fixed benchmark comparisons (namely, Section 5.3 with fixed self-sufficiency MPC, Section 5.4 with fixed cost MPC, and Section 5.5 with fixed multiobjective optimisation PSO), this section presents a new benchmark for adaptive weighting optimisation to clarify the benefits of AMPC further.

The logic governing the adaptive weighting factors in this PSO strategy mirrors the philosophy defined for the AMPC framework in Section 3.2.3. Specifically, the optimisation dynamically adjusts the priority of the objective function based on the market context: when the grid electricity price (C_{GRID}) exceeds the local generation cost ($C_{P,i,k}$), the weighting factors are shifted to prioritise self-sufficiency, compelling the EC to rely on prosumers' resources. Conversely, when $C_{GRID} < C_{P,i,k}$, the weight on economic cost maximisation is increased, as in Eq. (20), encouraging the primary grid's participation in demand coverage and consequently reducing the dispatch burden on prosumers.

The results of this adaptive strategy are illustrated in Fig. 13. In Fig. 13a, focusing on the power balance, the ECs' response to price signals is evident. During high-price intervals (0–50 s, 100–150 s, and 200–250 s), demand is entirely met by prosumers' aggregate generation, resulting in zero energy exchange with the main grid. However, during periods where the grid price drops below the local generation cost, the weighting factor shift triggers a substantial injection of grid power. This is observed in the interval 50–100 s, with a grid participation of 450 kW, and most notably between 150 and 200 s, where grid imports peak at 527 kW. This behaviour stands in sharp contrast to the AMPC scenario (Fig. 8), where the grid contribution was modulated more conservatively between 200 and 230 kW during similar price conditions.

While higher grid participation during low-price scenarios theoretically represents a direct economic benefit for the EC operation, it introduces significant technical inefficiencies, as evidenced in the subsequent subplots. Fig. 13b shows that high-power flows from the primary grid led to a substantial surge in generation losses. Specifically, in the intervals 50–100 s and 150–200 s, the losses spike to approximately 50 kW, a value considerably higher than that observed in strategies prioritising local consumption.

Furthermore, regarding the utilisation of installed capacity shown in Fig. 13c, it is observed that during periods when the primary grid is the dominant supplier, reliance on internal assets diminishes. The utilisation

Table 5
Comparative performance of AMPC against SS-MPC, EB-MPC and PSO-EMS.

Parameter	Description	AMPC	SS-MPC	EB-MPC	PSO-EMS	Adaptive PSO
$C^{tot}_{op,k}$	Mean total cost (€/h)	19.58	22.3 (+13.89%)	21.99 (+12.31%)	20.78 (+6.13%)	19.61 (+0.15%)
$P^{tot}_{loss,k}$	Mean total power generation losses (kW)	11.02	15.97 (+44.92%)	14.93 (+35.48%)	12.54 (+13.79%)	24.46 (+121%)
$U_{f,k}$	Mean utilisation factor (%)	79.31	78.95 (+0.45%)	68.73 (+13.34%)	81.32 (−2.53%)	56.84 (+28.33%)

factor drops to its minimum, ranging from 0.19 to 0.23. This highlights a critical deficiency of the adaptive multi-objective strategy when compared to the AMPC approach. While the adaptive PSO responds correctly to the instantaneous price signal, it lacks the prediction horizon to smooth the transition, leading to an "all-or-nothing" behaviour. In contrast, the AMPC anticipates future constraints, maintaining a more balanced utilisation of local assets to ensure stability and reduce the abrupt stress on the network, preventing the massive displacement of renewable generation observed here.

Moreover, Fig. 13d provides a breakdown of the total operational costs for the adaptive PSO. It is clear that during the maximum grid injection intervals (50–100 s and 150–200 s), the grid exchange and associated loss costs are the dominant components of total expenditure. This demonstrates that the aggressive exploitation of low spot prices incurs a secondary financial penalty through increased transmission inefficiencies, revealing that a strategy focused solely on price arbitrage ultimately compromises overall system efficiency relative to balanced local dispatch.

Finally, a quantitative analysis highlights the adaptive strategy's structural limitations. Although the adaptive PSO achieves an operational cost of 19.61 €/h—practically identical to the AMPC's 19.58 €/h (0.15% difference)—this economic parity comes at a severe technical cost. Generation losses under the adaptive PSO surge to 24,460 W, representing a 121.96% increase compared to the 11,020 W achieved by the AMPC. Furthermore, the capacity utilisation factor drops to 56.84, a 28.33% decrease from the 79.31 maintained by the predictive framework. These figures demonstrate that while the adaptive strategy performs instantaneous price arbitrage, it fails to optimise system efficiency, underscoring the necessity of the AMPC's predictive horizon. Table 5 presents a comparison between the AMPC and the different MPC strategies analysed.

6. Conclusions

This paper presented a novel AMPC framework for the intelligent management of prosumer-based ECs. The proposed AMPC was explicitly designed to navigate the complex trade-offs between economic viability, technical efficiency, and sustainable operation. The comprehensive comparative analysis conducted in this study confirmed the superiority of the adaptive approach over conventional control paradigms. When benchmarked against fixed-priority strategies, the AMPC demonstrated profound improvements. It achieved a significant 13.89% reduction in operational costs compared to an SS-MPC and a 12.31% reduction against an EB-MPC. Crucially, these economic gains were realised alongside massive reductions of 44.92% and 35.48% in power losses, respectively, proving the inherent inefficiency of rigid, non-adaptive control philosophies. Most remarkably, the AMPC even enhanced the average RET utilisation by 13.34% compared to the purely economic controller, proving that its intelligent strategy is not a mere compromise but a synergistically superior solution. Furthermore, the AMPC's performance was validated against a state-of-the-art, non-predictive PSO-EMS. This comparison highlighted the immense value of predictive control. The AMPC delivered a more balanced and effective solution, reducing average costs by 6.13% and losses by 13.79% with only a negligible 2.53% trade-off in the RET utilisation factor. Finally, the benchmark against the adaptive PSO revealed that while attaining economic parity, the AMPC avoided the 121.96% increase in power losses and the 28.33% reduction in available capacity utilisation. This empirically demonstrates that an aggressive, non-predictive pursuit of RET maximisation results in a financially and technically inefficient outcome, and that the AMPC's ability to anticipate future conditions enables it to avoid such penalties. These findings underscore the critical need for high-resolution, dynamic control strategies. Traditional energy management approaches based on course, hourly, or monthly optimisation horizons are fundamentally ill-equipped to handle the volatility of renewable generation and the dynamics of electricity markets. By operating on a much shorter timescale, the AMPC was able to capitalise on fleeting economic opportunities and react to sudden generation changes that conventional models would miss. In conclusion, this work demonstrated that an adaptive and predictive control paradigm was a practical approach for the robust and efficient operation of modern ECs, offering a demonstrably superior method for balancing economic, efficiency, and sustainability objectives.

CRediT authorship contribution statement

Pablo Horrillo-Quintero: Writing – original draft, Visualization, Validation, Software, Resources, Methodology, Investigation, Formal analysis, Data curation, Conceptualization. **Pablo García-Triviño:** Writing – original draft, Visualization, Validation, Software, Resources, Methodology, Investigation, Conceptualization. **Sérgio F. Santos:** Writing – original draft, Visualization, Validation, Resources, Methodology, Investigation, Conceptualization. **David Carrasco-González:** Writing – original draft, Visualization, Validation, Resources, Methodology, Investigation, Conceptualization. **Luis M. Fernández-Ramírez:** Writing – review & editing, Writing – original draft, Visualization, Validation, Supervision, Project administration, Methodology, Investigation, Funding acquisition, Conceptualization. **João P.S. Catalão:** Writing – original draft, Methodology, Investigation, Formal analysis, Conceptualization.

Declaration of competing interest

The authors declare that they have no known competing financial interests or personal relationships that could have influenced the work reported in this study.

Acknowledgments

The research leading to these results has received partial financial support from the Ministerio de Ciencia, Innovación y Universidades, Agencia Estatal de Investigación, FEDER, UE (Grant PID2024-156036OB-C32 supported by MCIN /AEI /10.13039/501100011033 /FEDER, UE) and from the Consejería de Universidades, Investigación e Innovación de la Junta de Andalucía (Grant DGP_PIDI_2024_02368). The work of Pablo Horrillo-Quintero was partially supported by the Fundación Campus Tecnológico de Algeciras, with funding provided by the Consejería de Universidades, Investigación e Innovación de la Junta de Andalucía and the 'PLAN PROPIO-UCA 2025-2027' program. Moreover, J.P.S. Catalão acknowledges support from the EU Horizon Europe Programme under GA ID: 101230578 (INNO-TREC Project; DOI: 10.3030/101230578) and from COMPETE2030-FEDER-00883700 and

FCT (INVINCIBLE Project; DOI: 10.54499/2023.17788.ICDT).

Data availability

Data will be made available on request.

References

[1] Lazaroiu AC, Roscia M, Lazaroiu GC, Siano P. Review of energy communities: definitions, regulations, topologies, and technologies. Smart. Cities 2025:8. https://doi.org/10.3390/smartcities8010008.

[2] Li L, Fan S, Xiao J, Zhang Y, Huang R, He G. Energy management strategy for community prosumers aggregated VPP participation in the ancillary services market based on P2P trading. Appl Energy 2025:384. https://doi.org/10.1016/j.apenergy.2025.125472.

[3] Foroughi M, Bagherpour M, Eliassen F, Poudineh R. Autonomy as empowerment: a taxonomic framework for analysing energy autonomy in local flexibility markets. Appl Energy 2025:389. https://doi.org/10.1016/j.apenergy.2025.125777.

[4] Tsao YC, IgG Arei Banyupramesta, Lu JC. Optimising grid energy management through the integration of inverter-based resources and community energy prosumers for sustainable energy systems. Energ Conver Manage 2025:344. https://doi.org/10.1016/j.enconman.2025.120265.

[5] Ghanavati F, Osório GJ, Matias JCO, Catalão JPS. Transactive data-driven and consumer-centric home energy management system for local energy communities in Portugal. Sustain Cities Soc 2025:131. https://doi.org/10.1016/j.scs.2025.106698.

[6] Petrovich C, Branchetti S, D'Agosta G. Parametrization of self-consumption and self-sufficiency in renewable energy communities: a case study application. Energy Ecol Environ 2025;10:324–51. https://doi.org/10.1007/s40974-025-00353-z.

[7] Diahovchenko I, Petrichenko L. Assessment of energy losses in power distribution systems with individual prosumers and energy communities. The Journal of Engineering 2023;2023. doi:https://doi.org/10.1049/tje2.12243.

[8] Dimovski A, Moncecchi M, Merlo M. Impact of energy communities on the distribution network: an Italian case study. Sustainable Energy, Grids and Networks 2023:35. https://doi.org/10.1016/j.segan.2023.101148.

[9] Ergun S, Dik A, Boukhanouf R, Omer S. Large-scale renewable energy integration: tackling technical obstacles and exploring energy storage innovations. Sustainability (Switzerland) 2025:17. https://doi.org/10.3390/su17031311.

[10] Seylab MR, Naderi MS, Gharehpetian GB. Dynamic energy management and control of networked microgrids based on load to grid services and incentive-based demand response programs: a multi-agent deep reinforcement learning approach. Sustain Cities Soc 2024:117. https://doi.org/10.1016/j.scs.2024.105957.

[11] Sepehrzad R, Yadav M, Lazaroiu GC, Avramidis II, Benitez IB, Di Somma M, et al. A critical overview of local energy communities: state-of-the-art, real-life applications & challenges and tackling the academia-industry gap. Renew Sustain Energy Rev 2026:226. https://doi.org/10.1016/j.rser.2025.116165.

[12] Basilico P, Biancardi A, D'Adamo I, Gastaldi M, Yigitcanlar T. Renewable energy communities for sustainable cities: economic insights into subsidies, market dynamics and benefits distribution. Appl Energy 2025:389. https://doi.org/10.1016/j.apenergy.2025.125752.

[13] Selim A, Mo H, Pota H. Optimization framework for multi-vector energy communities with uncertainty-aware energy management. Appl Energy 2025:395. https://doi.org/10.1016/j.apenergy.2025.126145.

[14] Dorahaki S, MollahassaniPour M, Rashidinejad M, Muyeen SM, Siano P, Shafie-Khah M. A robust optimization approach for enabling flexibility, self-sufficiency, and environmental sustainability in a local multi-carrier energy community. Appl Energy 2025:392. https://doi.org/10.1016/j.apenergy.2025.125997.

[15] dos Santos SAB, Coutinho LRR, Tofoli FL, Barroso GC. Community energy management system for residential energy communities integrating demand response, distributed generation, and energy storage systems. J Energy Storage 2025:132. https://doi.org/10.1016/j.est.2025.117832.

[16] Khojasteh M, Faria P, Vale Z. Adaptive robust strategy for energy and regulation Service Management in Local Energy Communities. Appl Energy 2025:377. https://doi.org/10.1016/j.apenergy.2024.124648.

[17] Casella V, Ferro G, Parodi L, Robba M. Maximizing shared benefits in renewable energy communities: a Bilevel optimisation model. Appl Energy 2025:386. https://doi.org/10.1016/j.apenergy.2025.125562.

[18] Khojasteh M, Faria P, Vale Z. Distributed robust optimisation model for resiliency analysis of energy communities with shared energy storage systems. Energy 2025:320. https://doi.org/10.1016/j.energy.2025.135337.

[19] Putratama MA, Rigo-Mariani R, Mustika AD, Debusschere V, Pachurka A, Besanger Y. A three-stage strategy with settlement for an energy community management under grid constraints. IEEE Trans Smart Grid 2023;14:1505–14. https://doi.org/10.1109/TSG.2022.3167862.

[20] Brusco G, Menniti D, Sorrentino N. A rolling horizon management model to reduce imbalance in real-time for a renewable energy community. Sustainable Energy, Grids and Networks 2025:43. https://doi.org/10.1016/j.segan.2025.101828.

[21] Dao LA, Dehghani-Pilehvarani A, Markou A, Ferrarini L. A hierarchical distributed predictive control approach for microgrids energy management. Sustain Cities Soc 2019:48. https://doi.org/10.1016/j.scs.2019.101536.

[22] Sivianes M, Maestre JM, Zafra-Cabeza A, Bordons C. Blockchain for energy trading in energy communities using stochastic and distributed model predictive control. IEEE Trans Control Syst Technol 2023;31(5):2132–45. https://doi.org/10.1109/TCST.2023.3291635.

[23] Xie P, Wang H, Jia Y. Decentralized energy management regime for prosumer community microgrids using flexible tube model predictive control. Electr Pow Syst Res 2024:236. https://doi.org/10.1016/j.epsr.2024.110553.

[24] Zahraoui Y, Gros S, Rajasekharan J, Oleinikova I. Integration of energy communities via multi-level dynamic markets. In: International conference on the European energy market. EEM: IEEE Computer Society; 2025. https://doi.org/10.1109/EEM64765.2025.11050128.

[25] Tang H, Li B, Zhang Y, Pan J, Wang S. A coordinated predictive scheduling and real-time adaptive control for integrated building energy systems with hybrid storage and rooftop PV. Renew. Energy 2025:239. https://doi.org/10.1016/j.renene.2024.122047.

[26] Ishibashi T, Furukakoi M, Uehara A, Masrur H, Rashwan A, Krishna N, et al. Model predictive control based optimal operation of smart city. Sustain Cities Soc 2024:114. https://doi.org/10.1016/j.scs.2024.105759.

[27] Mathworks "Tune Weights". Online, Accessed 15-Sept-2025, Available https://www.mathworks.com/help/mpc/ug/tuning-weights.html.

[28] Sarmadi BK, Shayeghi H, Seyedshenava S, Shafie-khah M. Multiple microgrids intelligent energy management with capacity constraint using hybrid deep neural network and reinforcement learning. International Journal of Electrical Power and Energy Systems 2025:172. https://doi.org/10.1016/j.ijepes.2025.111179.

[29] Li LL, Ji BX, Li ZT, Lim MK, Sethanan K, Tseng ML. Microgrid energy management system with degradation cost and carbon trading mechanism: a multi-objective artificial hummingbird algorithm. Appl Energy 2025:378. https://doi.org/10.1016/j.apenergy.2024.124853.

[30] Chen B, Li Z, Liu B, Fan H, Zhong Q. Dynamic cooperative scheduling and adaptive benefit allocation for multi-microgrid systems with shared energy storage under source-load uncertainty. J Energy Storage 2025:128. https://doi.org/10.1016/j.est.2025.117213.

[31] Žnidarec M, Šljivac D, Knežević G, Pandžić H. Double-layer microgrid energy management system for strategic short-term operation scheduling. International Journal of Electrical Power and Energy Systems 2024:157. https://doi.org/10.1016/j.ijepes.2024.109816.

[32] Horrillo-Quintero P, García-Triviño P, Ugalde-Loo CE, Hosseini E, García-Vázquez CA, Tostado M, et al. Efficient energy dispatch in multi-energy microgrids with a hybrid control approach for energy management system. Energy 2025:317. https://doi.org/10.1016/j.energy.2025.134599.

[33] Koumaniotis EK, Kyriakou DG, Kanellos FD. Optimal and sustainable operation of energy communities organized in interconnected microgrids. Energies (Basel) 2025:18. https://doi.org/10.3390/en18082087.

[34] Cheng Y, Zheng H, Juanatas RA, Golkar MJ. Profitably scheduling the energy hub of inhabitable houses considering electric vehicles, storage systems, revival provenances and demand side management through a modified particle swarm optimization. Sustain Cities Soc 2023:92. https://doi.org/10.1016/j.scs.2023.104487.